frontiers in Remote Sensing

TYPE Original Research
PUBLISHED 11 March 2026
DOI 10.3389/frsen.2026.1659305

OPEN ACCESS

EDITED BY
Jane Southworth,
University of Florida, United States

REVIEWED BY
Emilio Ramírez-Juidías,
Universidad de Sevilla Instituto Universitario de Arquitectura y Ciencias de la Construccion, Spain
Damir Klobučar,
Croatian Forests Ltd. Zagreb, Croatia
Xiongwei Liang,
Harbin University, China

*CORRESPONDENCE
Audrey Mercier,
mercieraudrey2@gmail.com

RECEIVED 03 July 2025
REVISED 28 January 2026
ACCEPTED 09 February 2026
PUBLISHED 11 March 2026

CITATION
Mercier A, Betbeder J, Mortier F, Barbier N, Ploton P, Cornu G and Couteron P (2026) Mapping small-sized logging disturbances in tropical forests using Sentinel-1 time series and an extensive ground truth dataset.
Front. Remote Sens. 7:1659305.
doi: 10.3389/frsen.2026.1659305

Mapping small-sized logging disturbances in tropical forests using Sentinel-1 time series and an extensive ground truth dataset

Audrey Mercier[1,2,3,4]*, Julie Betbeder[1,2], Frédéric Mortier[3,5], Nicolas Barbier[3], Pierre Ploton[3,6], Guillaume Cornu[1,2] and Pierre Couteron[3]

[1]CIRAD, Forêts et Sociétés, Montpellier, France, [2]Forêts et Sociétés Unit, University Montpellier, CIRAD, Montpellier, France, [3]AMAP Unit, University Montpellier, IRD, CIRAD, CNRS, INRAE, Montpellier, France, [4]School of Engineering, Aalto University, Espoo, Finland, [5]Environmental Justice Program–Georgetown, Georgetown University, Washington, DC, United States, [6]Plant Systematics and Ecology Laboratory, Higher Teachers' Training College, University of Yaoundé I, Yaoundé, Cameroon

Deforestation and forest degradation are the main threats to biodiversity and carbon stocks in tropical forests. Advances in optical and SAR satellite sensors have enabled the development of real-time monitoring of deforestation on a global scale. SAR is particularly appealing in tropical areas due to its insensitivity to cloud cover. However, the automatic detection of small disturbed areas (such as individual tree felling gaps) remains a major challenge. Thanks to a unique dataset consisting of 23,759 locations of individual tree felling gaps and multi-date drone lidar acquisitions, we evaluated the potential of Sentinel-1 dense time series for monitoring small-sized forest disturbances substantially smaller than 0.1 ha on both FSC-certified and artisanal logging sites in the Congo Basin. We designed a new method for forest monitoring using the fused-lasso technique optimized to detect abrupt changes of at least 0.02 ha in Sentinel-1 time series using the fused-lasso technique (Fused-Lasso Change Detection, FLCD). We assessed our new method along with the Cumulative Sum (CuSum) that also proved promising for detecting small impacts, referring for the first time to precise disturbance dates over large areas. Both approaches reached similar rates of confirmed felling gaps that were similarly increasing with gap size, and similar rates of unconfirmed detected gaps. The FLCD method estimates the dates of tree felling more accurately in FSC-certified areas (–2 days difference for FLCD and –19 for CuSum on average). The effective resolution of the S-1 images limits detection for the smallest gaps, yet the approach can help detect and monitor degradation fronts. Fused lasso regression is relevant for modeling the temporal trajectories of the radar signal, which will allow taking advantage of both the increasing availability of UAV-borne data and the lengthening of the S-1 image series.

KEYWORDS
artisanal and certified logging, Congo basin, fused-lasso, Sentinel-1 SAR time series, tree-felling gap detection, tropical forest degradation

1 Introduction

Tropical forests are known to play a key role in many ecosystem services such as carbon sequestration, climate regulation, and biodiversity conservation (Saha, 2021). However, these ecosystems have undergone extensive deforestation and degradation in recent decades. Monitoring deforestation is fairly well understood; between 1990 and 2020, 420 M ha have been deforested worldwide (Food and Agriculture Organization of the United Nations, 2020). Forest degradation is more complex to characterize and monitor by remote sensing, although previous studies have highlighted its significant contribution to carbon emissions (Pearson et al., 2017; Qin et al., 2021). Degradation can be defined as a change in forest structure and composition that results in the reduction or loss of ecosystem services provided by forests. This process can occur in multiple forms and vary widely on both a temporal and a spatial scale (Putz and Redford, 2010; Ghazoul et al., 2015).

In the Congo basin, forest logging, including formal and informal operations, is a major driver of forest degradation (Tegegne et al., 2016; Vancutsem et al., 2020). Quite often, logging-induced forest degradation has proved to be a pathway toward deforestation, as degraded forests are vulnerable to additional destruction causes (e.g., fires) and are easier to clear for crops by small farmers (Vancutsem et al., 2020). Formal logging activities correspond to industrial logging in large-scale concessions allocated to corporations by governments, while informal activities refer to artisanal logging for domestic markets and often entails illegal operations (Kleinschroth et al., 2019). In the Congo Basin, 11% of the area under concessions was certified by the Forest Stewardship Council (FSC) in 2016 (OFAC, 2023) requiring them to meet defined social and environmental standards for sustainable forest management (Kleinschroth et al., 2019). This includes reducing the size of felling gaps as part of reduced-impact logging techniques (RIL). In contrast, artisanal logging follows no specific standards but provides important income and employment opportunities for local communities (Lescuyer et al., 2025). It involves the manual felling and processing of trees by individual operators with limited resources and equipment (i.e., chainsaws, axes and hand saws). Artisanal harvesting of trees usually lead to small-sized felling gaps (i.e., <0.1 ha) located close to roads or rivers to limit transport costs (Lescuyer et al., 2013). Even though reduced-impact logging techniques (RIL) or certification have proven efficient to decrease detrimental effects on forest ecosystems (Putz et al., 2008), the majority of forest logging across the Congo basin is not certified and a substantial share of it does not comply with RIL principles. In the Democratic Republic of the Congo, 90% of all logging is estimated to be conducted in the informal sector, outside of registered logging concessions (Lawson, 2014). Recognizing and regulating artisanal logging could improve governance, secure incomes, and integrate local actors into sustainable forest management schemes (Lescuyer et al., 2025). To better characterize forest degradation, it is now crucial to enhance our ability to monitor both industrial (certified or not) and artisanal logging activities. This requires detecting small-sized forest disturbances, such as canopy gaps <0.1 ha.

The last two decades have been marked by the development of methodologies using optical satellite images to detect deforested and degraded areas by taking advantage of the long-term archives of Landsat imagery (Asner et al., 2005; Souza et al., 2005; Dutrieux et al., 2015; DeVries et al., 2015; Hansen et al., 2016; Vancutsem et al., 2020). Since the launch of the Sentinel-2 constellation in 2014, optical data with higher spatio-temporal resolutions are available and allow finer detection of forest disturbances (Zhang et al., 2021). The Global Land Analysis & Discovery (GLAD) Alert (Hansen et al., 2016), the Continuous Change Detection and Classification (Bullock et al., 2020) and the Tropical Moist Forest (TMF) (Vancutsem et al., 2020) are well known global operational systems to monitor forest degradation from a monthly to an annual basis. However, optical-based monitoring methods display limitations in tropical regions, as frequent cloud cover prevents the sensor from observing the land surface. They require clear images and dense time series with sufficient spatial resolution to detect the rapid changes in forest cover typical of forest degradation – particularly tree felling associated with FSC practices, Reduced Impact Logging (RIL), or small-scale artisanal activities – which create small canopy gaps that quickly regenerate through natural vegetation growth (Webb, 1997; Gourlet-Fleury et al., 2013; Dalagnol et al., 2019).

Synthetic Aperture Radar (SAR) sensors represent the most promising tools to address this challenge as the radar signal is not significantly affected by atmospheric conditions and can be acquired day or night. With its high spatio-temporal resolution and open-access data policy, the open-access Sentinel-1 (S-1) mission provides SAR satellite image time series that have demonstrated a high potential to monitor forest disturbances in tropical areas (Bouvet et al., 2018; Antropov et al., 2016; Mermoz et al., 2021; Ygorra et al., 2021; Reiche et al., 2021; Reiche et al., 2015; Aquino et al., 2022; Nolan, 2022; Bullock et al., 2022). For that purpose, the main methodological approach consists of detecting changes in the temporal radar signal of a forest canopy. Antropov et al. (2016) focused on the variations in the local standard deviation of VV and VH backscatter change. Reiche et al. (2015, 2021) developed an anomaly-detection method based on Bayesian update theory using VV polarization. Another methodological line consists in detecting the appearance of radar shadows (i.e., dark areas in radar images where the signal is blocked by tall objects) between intact and disturbed forest edges using a radar change ratio (Bouvet et al., 2018; Mermoz et al., 2021; Carstairs et al., 2022). For instance, Mermoz et al. (2021) computed a radar change ratio and compared its average value across the three last acquisitions against its historical baseline to detect changes. The present state of the art in forest monitoring tools based on S-1 time series allows mapping canopy gaps of sufficient individual size in nearly real time. Notably, the RAdar for Detecting Deforestation (RADD) system provides weekly alerts over most of the humid tropical forests for impacted areas larger than 0.1 ha (i.e. 1000 m^2 or 20 × 50 m). This fits to the detection of most deforestation spots linked to agriculture, mining or infrastructures.

To date, the detection of tree fall gaps, along with other small-sized forest disturbances <0.1 ha, that underlies forest degradation remains a major challenge (Dupuis, 2023; Aquino et al., 2022; Carstairs et al., 2022). Specifically, informal and artisanal logging calls for adequate methods to be monitored with sufficient spatiotemporal accuracy to detect developing degradation fronts. Whatever the type of logging, maps of small-sized forest disturbances are essential to ensure compliance with forestry

regulations and help in assessing and comparing the environmental impacts of the different kinds of logging, as to drive them towards the most sustainable approaches. Mapping of accurate forest disturbance dates is also crucial for monitoring sustainability criteria. For example, accurate dates could help control the legality of logging activities, which should occur during dry seasons to reduce soil damage (Putz and Pinard, 1993). In Central Africa, most forests already impacted by either RIL or informal logging remain mapped as 'intact' on currently available global products such as RADD alerts (Reiche et al., 2021), the TMF annual changes data (Vancutsem et al., 2020) and the Global Land Analysis & Discovery data (Potapov et al., 2020). In a FSC area in Peru, Aquino et al. (2002) have shown that RADD alerts were able to detect clear cuts (i.e., roads and log landing places), but missed the majority of the small-scale disturbances corresponding to selective felling, resulting in only 2% of logging disturbances detected. Most felling gaps are indeed far smaller than 0.1 ha in FSC and artisanal logging areas. The Cumulative Sum (CuSum) method has been introduced for detecting small-sized forest disturbances <0.1 ha (Aquino et al., 2022). These authors demonstrated that the CuSum outperformed the RADD system for the detection of small-sized forest disturbances (<0.1 ha) in dense tropical forests, and yielded high detection probability (78% in Gabon and 65% in Peru). However, while the CuSum method was validated on relatively small areas compared to the scale of tropical forest concessions, no evaluation was carried out concerning its ability to accurately detect the timing of tree felling events. Overall, monitoring small-sized forest disturbances is a technical challenge that is crucial for environmental conservation and sustainable forest management.

In the present study, we revisit the state of the art about using S-1 time series to detect small-sized canopy disturbances (i.e., <0.1 ha) and estimate disturbance dates, by introducing a new method and by taking opportunity of an exceptionally large dataset from different parts of the Congo basin (in three countries). The dataset entails both an exhaustive assessment of canopy disturbances from UAV-borne diachronic canopy altimetry (over 374 ha) and exhaustive censuses of felled-trees locations and dates for 23,759 tree felling events (in five FSC logging sites). In addition to extensive ground truth datasets collated by FSC-certified companies as part of their regulatory duty, the present study makes the first ever foray concerning felling gaps from artisanal logging, thanks to a dedicated field sampling. Our new method, hereafter referred to as Fused-Lasso Change Detection (FLCD) is built on fused-lasso regressions, a model-based approach demonstrating high potential in several fields, such as meteorology (Jeon et al., 2016) and signal regularization (Banerjee, 2022) by providing piecewise constant solutions (Tibshirani et al., 2005). Because the main trend of C-band SAR time series is expected to be roughly constant over time for intact forest canopies (Woodhouse et al., 1999), the fused-lasso method is hypothesized to be adequate for modeling abrupt change due to punctual disturbances in otherwise stable signal. The stationarity of the signal before and after disturbance is also a key assumption of the CuSum method (Aquino et al., 2022). On this basis, we address the following research questions:

- Can FLCD improve the detection of small-sized canopy disturbances in terms of dating accuracy and detection rates for both confirmed and unconfirmed events, and how does it compare to CuSum?
- How does the size of individual disturbances affect the detection accuracy and precision of both methods, and to what extent is this influenced by the inherent limitations of S-1 data?

Both FLCD and CuSum were relevant for mapping forest disturbances smaller than the state of the art (i.e., <0.1 ha), with CuSum slightly better at detecting disturbances and FLCD providing more accurate estimates of tree-felling dates. These complementary methods capture different aspects of forest degradation and offer a practical framework for monitoring small-scale disturbances in tropical forests on an annual basis, introducing new approaches for FSC and RIL logging monitoring and enabling the early detection of advancing degradation fronts in tropical landscapes that often precede deforestation.

2 Materials and methods

2.1 Study areas

The study was carried out in five sites (experiencing either FSC industrial or artisanal logging) located in three countries across the Congo Basin: the Republic of the Congo, the Democratic Republic of the Congo and Cameroon (see Figure 1). In all sites, two dry seasons (June - August and December - February) alternate with two wet seasons (March-May and September-November) during the year (Creese et al., 2019).

The two studies areas experiencing industrial logging are named Kabo (Kab, 2°34′N,17°08′E) and Mbeti (Mbe, 1°98′N,16°02′E) and are located in the northern part of the Republic of the Congo (see Figure 1) in a semi-deciduous tropical forest dominated by medium wood density tree species (Réjou-Méchain et al., 2021). They cover 2,953 km^2 and 5,650 km^2, respectively, and are exploited by a company named "Congolaise Industrielle des Bois" (CIB-Olam Concession), certified by the Forest Stewardship Council (FSC). The mean annual temperature at both sites is 25 °C and the mean annual precipitation is around 1,600 mm (Loubota Panzou et al., 2018). According to the overall inventory of forest stands in forest management units encompassing the two study areas, the average tree density was about 350 trees per ha, while basal area and above ground biomass were of 28 m^2/ha and 433 Mg/ha, respectively (Forni et al., 2019; Gourlet-Fleury et al., 2023).

The three study areas subjected to artisanal logging are named Yanonge (Yan, 0°49′N,24°7′E), in the Democratic Republic of the Congo, Mindourou (Min, 3°50N, 13°44E) and Dzeng (Dzg, 3°7′N, 11°82′E) in Cameroon and cover 155, 106 and 357 km^2, respectively (see Figure 1). The Yan and Min sites are located in a semi-deciduous evergreen transition forest (Réjou-Méchain et al., 2021). The Dzg site is located in a degraded semi-deciduous forest (Réjou-Méchain et al., 2021). The mean annual temperature is around 25, 23 and 23 °C in Yan, Min and Dzg respectively and the mean annual precipitation is around 1,800, 1,500 and 1700 mm respectively (climate-data.org).

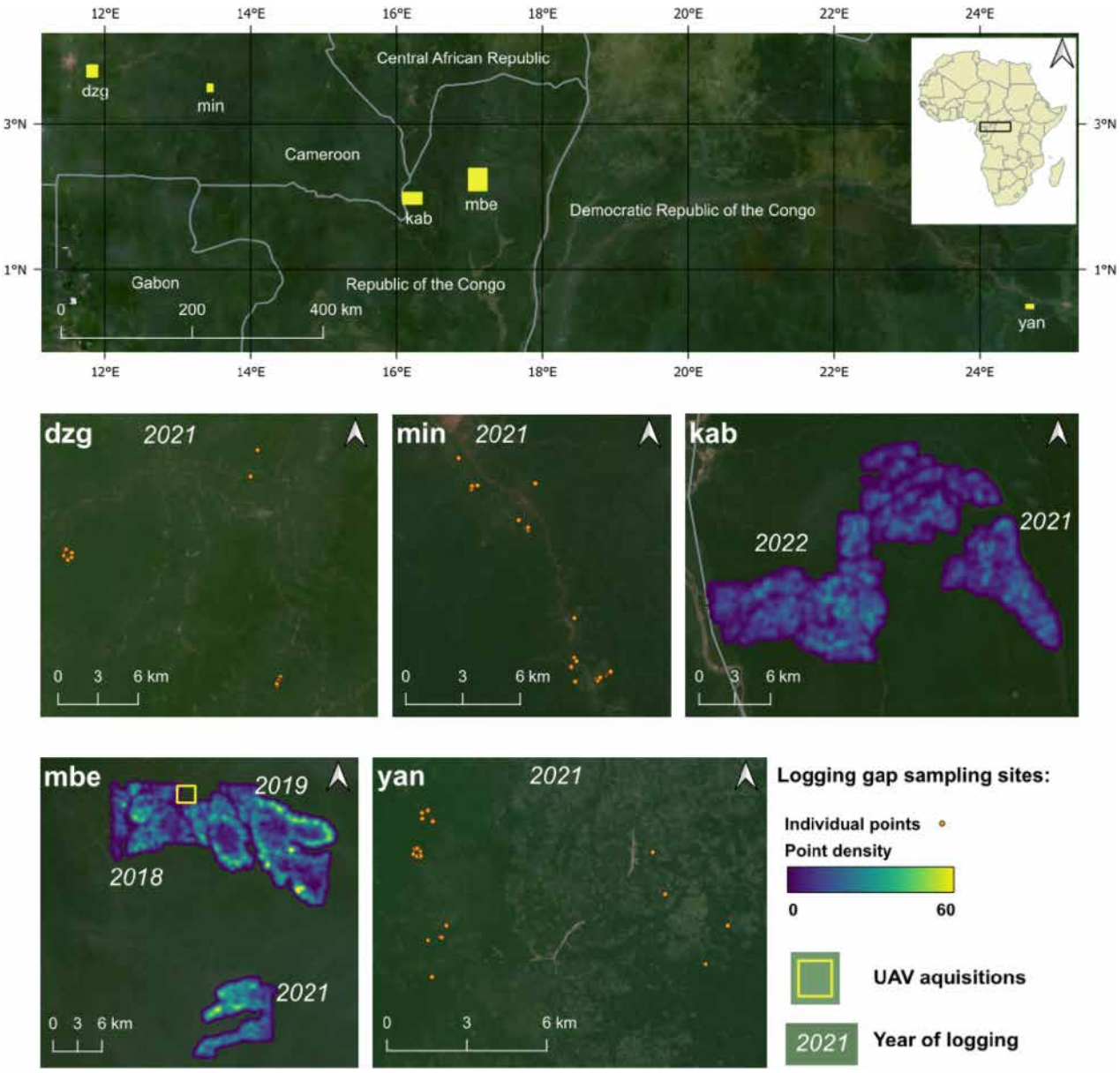

FIGURE 1
Location of the logging gap samples in the five study areas: dzg, min, kab, mbe and yan correspond to Dzeng, Mindourou, Kabo, Mbeti and Yanonge sites, respectively. The "mbe" panel shows the area covered by the UAV acquisitions. Sources: RGB basemap is a PlanetScope Tropical Normalized Analytic Biannual Archive from December 2019 (Planet Team, 2017) and administrative boundaries are from the Central African Forest Observatory (https://www.obsersurfacesandvatoire-comifac.net/).

2.2 UAV-derived binary forest disturbance map

Over the site of Mbe (Republic of the Congo), we had access to a detailed 3D representation of canopy disturbances thanks to repeated UAV surveys. Two main data sources were used and combined: stereophotogrammetry and LiDAR. RGB imagery data were acquired on 2018-06-18 and 2019-04-05 using a Ebee Sensefly fixed wing UAV. Stereophotogrammetric processing was performed using Pix4D software. Digital Surface Models were produced at a 0.1 m resolution. LiDAR acquisition was performed on 2020-02-13 using a Surveyor Ultra (Yellowscan) LiDAR sensor. The system comprises a VLP32 scanner (Velodyne) and an Applanix 15 IMU. The scanner was carried onboard a DJI Matrice 600 UAV with scanning direction perpendicular to flight direction, at a flight altitude of ~70 m above ground level (following SRTM DTM) and a flight speed of 15 m s^{-1}. An interline distance of 80 m was chosen to achieve ~50 % overlap at less than 45° incidence angle at actual ground level (which is below the SRTM altitude in a dense canopy). Differential correction of flight trajectories was achieved using an Emlid Reach RS2 GNSS base station on a point of location determined using a Precise Point Positioning approach using a full day of acquisition data. Post Processing Kinematic adjustment and optimisation of the trajectories was performed using the Applanix PosPac UAV software (v. 8.5). Las

point clouds were exported using CloudStation software (Yellowscan) on the basis of the optimized trajectories and sensor calibrated geometry. A digital surface model (DSM) was derived at 0.6 m horizontal resolution using the Lastools software function lasgrid, with the -max option. The description of the LiDAR acquisitions are detailed in Kaçamak et al. (2022).

The total overlap area between the three surveyed dates was ~374 ha. To ensure perfect spatial adjustment, a global and local adjustment was performed using the Arosics software (Scheffler et al., 2017) using the LiDAR coverage as reference. Two binary maps of small-sized forest disturbance/non disturbance were derived from the three resulting DSM. Disturbed pixels were defined as a decrease in tree canopy equal or higher than 10 m between 2019-2018 and 2019-2020. To compute the 2019-2020 disturbances, the DSM of 2019 was resampled to the spatial resolution of the 2020 DSM (0.6 m). Some pixels were classified as disturbed because of very slight spatial shifts between the DSMs. Therefore, a morphological opening operation was applied using the Binary Morphological Operation algorithm from OTB (Grizonnet et al., 2017). An erosion operation was used to remove disturbance patches smaller than 2 m, followed by a dilation of 2 m to restore the size of the remaining disturbances. Despite the differences in sensitivity to forest cover between LiDAR and stereophotogrammetry data (Goodbody et al., 2019), the use of the DSM instead of points clouds and the removal of very small detections avoid biased in UAV-derived binary forest disturbance maps. The UAV-derived binary forest disturbance maps were finally resampled to 1 m resolution to limit time-computing.

FLCD and CuSum were trained on the UAV-covered footprint and validated on the remaining Mbe area and on the five other study sites using independent GPS-based datasets. The UAV-derived binary disturbance map is available only for the Mbe site, which limits its representativeness across the full range of forest types considered in this study. However, Mbe and Kab share comparable forest types and climatic conditions, so this limitation is expected to have a limited impact on method performance in FSC-certified sites, while potentially affecting performance in the three artisanal logging sites (see Section 2.1).

Several sources of uncertainty are inherent to UAV-based canopy disturbance mapping. Time intervals between acquisitions (2018–2019 and 2019–2020) do not allow precise dating of individual tree-felling events. DSMs derived from RGB stereophotogrammetry can also be affected by illumination conditions, cloud shadows and variations in light diffusion within the canopy, introducing local height estimation errors. These effects were mitigated by focusing on large canopy height losses (≥10 m) and the UAV acquisitions were all performed under clear weather conditions.

2.3 GPS locations of felled trees

This dataset includes coordinates (EPSG: 4,326) of felled trees and associated felling date recorded in FSC (Mbe and Kab) and artisanal logging areas (Yan, Dzg, and Min).

Contrary to the previous dataset, spatial extents of disturbances were not available. Only the location of the felled trees stumps were provided and analyzed.

2.3.1 FSC industrial logging

The GPS points were provided by the CIB-Olam operating in the Republic of the Congo. The FSC data include 6,561, 6,520 and 3,663 GPS points at the Mbe study area collected during annual campaigns in 2018, 2019 and 2021, respectively. In Kab, 3,779 and 3,279 GPS points of felled trees were collected during annual campaigns in 2021 and 2022, respectively. Dates of felling associated with the locations are accurate to the day. The locations of the trees were collected during the pre-felling inventory. In 2018 and 2019, the locations were determined relative to a regular 50 m grid materialized by sticks on the site. Since 2021, GPS points have been recorded using smartphones at the base of trees with an accuracy ranging from 20 to 25 m. Since uncertainty on GPS position is equal or above the S-1 genuine resolution of 20 × 22 m, reference polygons from the GPS points were computed by applying a buffer area of 20 m.

2.3.2 Artisanal logging

We conducted field surveys of artisanal logging sites in June 2021 and March 2022 in the Democratic Republic of the Congo and in November 2021 in Cameroon. The logging gaps locations were recorded in the middle of the felling gap with a GPS Garmin 60CXS (accuracy ranging from 3 to 10 m). The loggers provided the cutting dates accurate to the month. As these dates were based on retrospective declarations and were therefore subject to uncertainty, they were independently confirmed or corrected by visualizing the basemap series "PS Tropical Normalized Analytic Monthly" at a 4.77-m resolution from PLANET Explorer (Planet Team, 2017). Given that this study aims to assess both detection and timing accuracy, only disturbances with independently verifiable dates were included. When no canopy disturbance could be visually identified in the PLANET imagery, the corresponding logging gap was excluded from the validation dataset due to temporal uncertainty. Most excluded gaps corresponded to events reported as the oldest by the operators (2018–2020). In total, 22, 35 and 31 logging gaps dating from 2021 were selected from the field surveys conducted in Yan, Min and Dzg, respectively.

2.4 Sentinel-1 SAR time series

Over the five study areas, S-1 C-band (5.405 GHz) time series were acquired between 2018 and 2022 (Mbe: 2018-2019 and 2021, Kab: 2021-2022, Yan: 2021, Dzg: 2021 and Min: 2021). The images were downloaded in Interferometric WideSwath (IW) mode, corresponding to a resolution of 20 × 22m (rg×az), a pixel spacing of 10 × 10m (rg×az) and a swath of 250 km. The revisit frequency of the S-1 constellation is 12 days in Central Africa, increasing to 24 days from December 2021 onward due to the loss of data transmission from the S-1B satellite. This may reduce sensitivity to very short-term disturbances and affect the temporal accuracy of detection. However, logging gaps persist for several months to years before canopy closure, as shown by previous studies in Amazonia (Asner et al., 2004), which limits the impact of this longer revisit interval on disturbance detection. The Level-1 Ground Range Detected (GRD) products were used, which are multilook intensity (5 and 1 looks according to slant range and

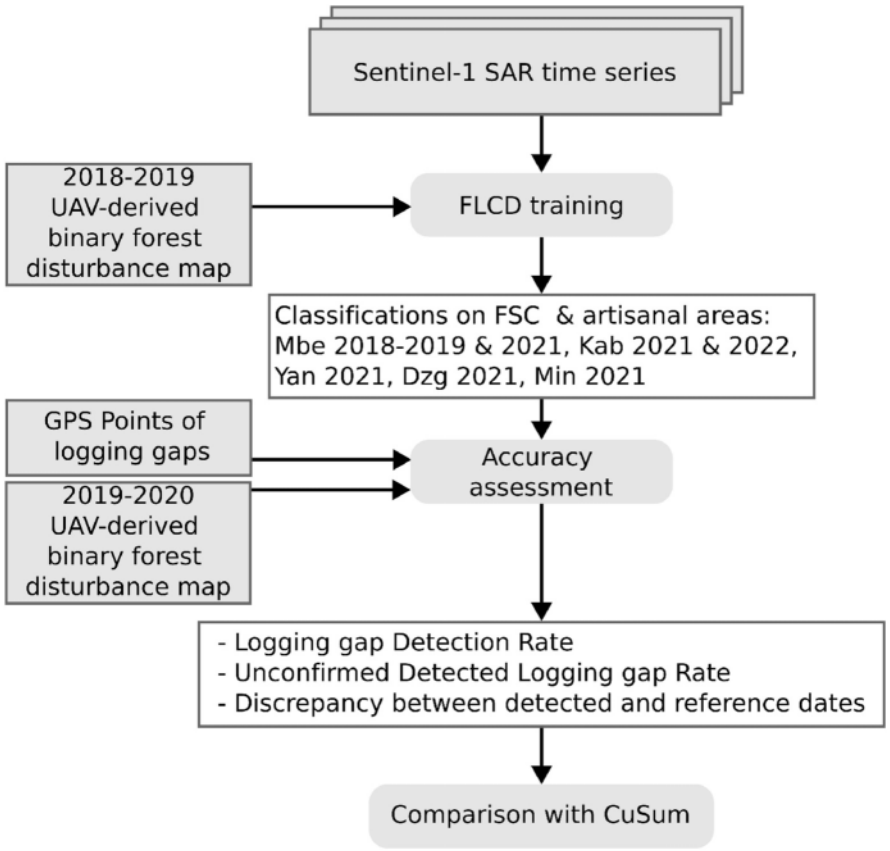

FIGURE 2
Workflow implemented in this study. Calibrating and validating the FLCD method using UAV-derived forest disturbance data, followed by validation in FSC and artisanal study areas.

azimuthal direction, respectively) projected to a ground range based on an Earth ellipsoid model. Since the S-1 satellite can only map our study areas in a single pass, images were acquired in descending mode for the study areas located in the Republic of the Congo and the Democratic Republic of the Congo (Mbe, Kab, Yan) and in ascending mode for the study areas located in Cameroon (Dzg, Min). All available images were downloaded from Google Earth Engine (GEE) "COPERNICUS/S1_GRD" collection using the open python code (https://github.com/chiaquino/S1_CuSum) provided by Aquino et al. (2022). For each observed year, the time series started 12 months before the year and ended 6 months after the observed year, e.g., for the year 2019, the time series extended from 2018-01-01 to 2020-06-01. Disturbance detection requires a post-disturbance series of 6 months for optimal results (Supplementary Appendix S5.1). Pre-processing already done on GEE "COPERNICUS/S1_GRD" collection includes thermal noise removal, radiometric calibration and terrain correction. Speckle filtering was not applied to either FLCD or CuSum. Aquino et al. (2022) showed that speckle filtering degraded the detection accuracy of CuSum. Similarly, internal analyses conducted for FLCD using Boxcar, Refined Lee, Lee, and Lee Sigma filters led to a slight increase in recall, but substantially reduced precision and increased false detections. Spatial filtering may alter the pixel backscatter signal, which is critical for detection of very small canopy gaps, while the lasso regression inherently accounts for noise. The python code from Aquino et al. (2022) further performs sigma nought to gamma nought (γ^0) conversion and data mosaicking for each unique date using the GEE mosaic function. The γ^0 corresponds to sigma nought corrected for near-far range incidence angle variations. It was selected since Hoekman et al. (2020) demonstrated that γ^0 was more relevant than sigma nought to monitor structural changes in tropical forests. Given the relatively flat terrain of the Congo basin, angle-based correction is sufficient to account for backscattering variations without needing a more complex area-based correction (Small, 2011). Our study focused on the VV polarization since Ygorra et al. (2021) found that the VV polarization was more accurate than VH to monitor tropical forest changes using S-1 data. A number of 72–84 γ^0 VV S-1 images was used, depending on the site. Images were projected in WGS84 coordinate system (EPSG: 4,326).

2.5 Fused-lasso change detection method (FLCD)

The FLCD method aims at producing a binary map featuring small-sized forest disturbances (associated with magnitude values), while putting emphasis of disturbance date assessment. Figure 2 illustrates the workflow implemented in this study. The Table 1 indicates the use of each dataset in the workflow.

TABLE 1 Datasets used in this study with their corresponding study area, logging type and year, data type, partition and number of samples. The sites correspond to Yanonge (Yan), in the Democratic Republic of the Congo, Mindourou (Min,) and Dzeng (Dzg) in Cameroon, and Kabo (Kab) and Mbeti (Mbe) in the Republic of the Congo. The logging type is Forest Stewardship Council certified (FSC) or artisanal logging.

Dataset name	Study area	Logging type	Logging year	Dataset type	Partition	Number of samples
2018-2019 UAV-derived Binary forest disturbance map	Mbe	FSC	2018	Raster	Traning	-
2019-2020 UAV-derived Binary forest disturbance map	Mbe	-	no logging	Raster	Validation	-
GPS points in Mbe 2018	Mbe	FSC	2018	GPS points	Validation	6,433
GPS points in Mbe 2019	Mbe	FSC	2019	GPS points	Validation	6,520
GPS points in Mbe 2021	Mbe	FSC	2021	GPS points	Validation	3,663
GPS points in Kab 2021	Kab	FSC	2021	GPS points	Validation	3,779
GPS points in Kab 2022	Kab	FSC	2022	GPS points	Validation	3,279
GPS points in Dzg 2021	Dzg	Artisanal	2021	GPS points	Validation	35
GPS points in Min 2021	Min	Artisanal	2021	GPS points	Validation	28
GPS points in Yan 2021	Yan	Artisanal	2021	GPS points	Validation	22

To produce maps of small-sized forest disturbances from the S-1 SAR time series, we developed a method we call Fused-Lasso Change Detection (FLCD). Figure 3 describes the main steps (detailed below) of the FLCD method. First, fused-lasso regressions are computed on pixelwise S-1 time series. Secondly, iterative local differences between successive lasso-smoothed values and corresponding sliding sums are applied to highlight signal decreases. Finally, a post-classification step (spatio-temporal filtering) based on the disturbance dates is applied to reduce false detections.

2.5.1 Fused-lasso regressions

The lasso (Tibshirani, 1996) has been widely used for selection and dimension reduction purposes in many applied fields. It consists of penalizing least squares regression by the sum of the absolute values of the coefficients (L-1 norm). This penalty shrinks toward zero parameters with small effects and thus favors sparse solutions. However, lasso does not consider underlying structures within series such as temporal order. The fused-lasso method (Tibshirani et al., 2005) was developed to overcome such limitations by penalizing the L-1 norm of coefficient successive differences (Banerjee, 2022):

$$\arg\min_{\mu} \frac{1}{2}\|y-\mu\|_2^2 + \lambda \sum_{t=2}^{T} |\mu_t - \mu_{t-1}|$$

where y is the observed signal for a given pixel over time T, μ_i its vector of mean parameters, λ a regularization parameter and $\|.\|_2$ the L_2-norm. Note, that pixels index have been omitted for clarity, but such optimization problem has been repeated for each pixel i.

Fused-lasso produces trend estimates that are piecewise linear and appeared relevant for the analysis of temporal signals with an underlying piecewise linear trend, changes in slope and abrupt changes.

To implement the fused-lasso method, we used the "fusedlasso1d", "cv.trendfiler" and "softthresh" functions from the "genlasso" R package (Arnold et al., 2022). The gamma value was set to 0 and the lambda value was determined by cross-validation according to the one standard error rule for each pixel. The lambda parameter controls the strength of the penalty on differences between consecutive coefficients, and therefore manages the smoothness of the lasso solution. In practice, high lambda values lead to stronger temporal smoothing in the fused lasso regression, whereas smaller lambda values produce more flexible solutions with frequent local variations leading to overdetection. Although it would have been possible to fix a single lambda for the entire study area, allowing it to vary per pixel improved precision.

2.5.2 From fused-lasso to mapping of small-sized canopy disturbances

For each S-1 pixel, we extracted the γ^0 values per date and computed fused-lasso regressions. A local difference between consecutive dates was calculated on the fused-lasso series. However, the resulting extreme negative values may extend over several months due to a gradual decrease in the C-band SAR signal (Reiche et al., 2018a; Hethcoat et al., 2021; Balling et al., 2023; Tang et al., 2023). Therefore, we summed the troughs over a sliding period, resulting in sliding sum values. Finally, the dates were classified as disturbed if the sliding sum values of the pixel fell below a detection threshold calculated from the distribution of all negative sliding sum values across the entire image. The size of the sliding sum window and the detection threshold were established during the training process (see Subsection 2.6).

For a given pixel, the actual disturbance date was defined as the first date the pixel was classified as disturbed in the time series. In addition, we defined and computed a "disturbance magnitude value" for each disturbed pixel based on VV backscatter values in decibels. Let us define τ_1 and τ_2 as the dates corresponding to the beginning and the end of disturbance period. This period corresponds to the consecutive dates classified as disturbed in the time series when the detection threshold is reached, i.e., when the summed negative values of the time series are more extreme than 99.99% of the corresponding values across all pixels. The magnitude of the disturbance, δ, is calculated as the difference between the median

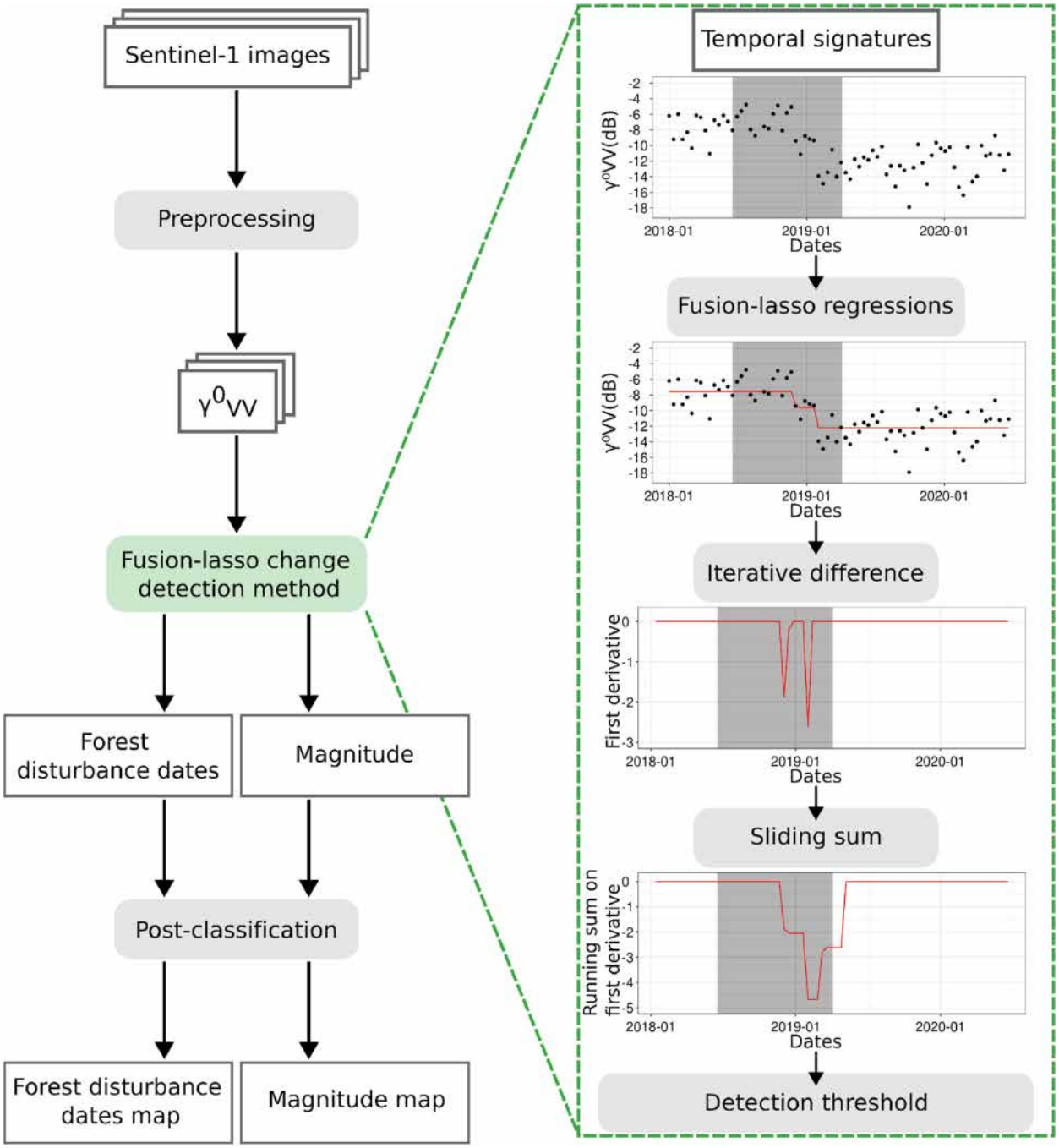

FIGURE 3
Operation flow for the Fused-Lasso Change Detection method. Grey rectangles on the right hand panel highlight the period monitored by UAV. Sentinel-1 images were downloaded and preprocessed to extract gamma nought from the VV polarization. Then, the fused lasso change detection method was performed on each pixel to produce maps of forest disturbance dates and disturbance magnitude. This included the following steps: 1) fitting fused lasso regressions on the temporal signature, 2) computing iterative differences 3) performing a 3-month sliding sum on the results 4) classifying pixels as disturbed based on a detection threshold corresponding to the 0.01th percentile of the negative sliding sum values on the image. Finally a post-classification step consisting of spatio-temporal filtering was applied.

of the VV signal over the 3 months preceding the first disturbance date τ_1 and the minimum of the signal between τ_1 and τ_2:

$$\delta = \gamma_0\left(\bar{y}_{(\tau_1-3):\,\tau_1)} - \min y_{\tau_1:\,\tau_2}\right)$$

where i: j denotes the sequence from an integer i to another j and γ_0 the gamma nought values for VV polarization.

2.5.3 Post-classification spatial analysis

We applied a final post-classification process aimed at decreasing false detections by conducting a spatio-temporal analysis from the forest disturbance dates map. Because the detection threshold is defined using the distribution of negative

sliding sum values over the entire image, a small number of individual pixels may be classified as disturbed even in intact forest areas. These false positives are typically linked to SAR signal noise that tend to be spatially isolated. To address this issue, detected pixels that did not exhibit spatial contiguity with at least one neighboring pixel detected as disturbed within a 15-day time interval were removed. Spatial contiguity was defined at the S-1 pixel spacing (10 m), and isolated single-pixel detections were excluded. This spatial filtering strategy was optimized using UAV-derived disturbance maps as ground truth. Therefore, the present implementation of the FLCD method cannot detect disturbances smaller than two adjacent 10 m pixels (i.e., 0.02 ha), unless such disturbances induce a strong enough decrease in the S-1 signal over both pixels, which remains possible given its effective spatial resolution (~20 × 22 m). Real disturbances not influencing more than one S-1 pixel (i.e., spatially isolated) may exist, notably, when relating to natural disturbances including branch falls or for small felling gaps. As a result, the method is designed to focus on detecting real canopy gaps, even if this implies missing small or isolated disturbances.

2.6 Training on the 2018-2019 UAV-derived binary forest disturbance map

The FLCD parameters (sliding period size for the sliding sum, detection threshold and exclusion patch size) were calibrated using the UAV-derived binary forest disturbance map (over 374 ha) for the 2018-2019 period in Mbe, the Republic of the Congo (see Supplementary Appendix S5.2). A 5-fold cross-validation approach was used to select the two FLCD parameters, namely, the detection threshold and the sliding sum window. Five training and testing datasets were defined within the UAV study area. FLCD were applied to each training and corresponding test dataset. The detection threshold was tested at values of 0.005, 0.01, and 0.015; the sliding window length at 30, 60, 90, and 120 days. For each parameter configuration, the mean performance and confidence intervals were computed across the five train–test splits (Supplementary Appendix S5.2).

The reference polygons were rasterized on the basis of the detected disturbance maps grid (10 m resolution). Then, we assessed the FLCD classifications computing precision (Equation 1) and recall (Equation 2), which are suitable when focusing on small proportions of positive class, using the following equations.

$$\text{precision} = \frac{\text{TP}}{\text{TP} + \text{FP}} \tag{1}$$

$$\text{recall} = \frac{\text{TP}}{\text{TP} + \text{FN}} \tag{2}$$

where TP = true positive, FP = false positive and FN = false negative.

The parameters yielding the best compromise between a high precision and a high recall were selected.

2.7 Validation on extended areas using GPS points

The trained FLCD method was validated on extensive FSC and artisanal areas using the felled-trees locations dataset. GPS points have two main limitations: they only indicate felled trees without providing data on non-disturbed pixels, and the spatial discrepancies between GPS points taken near stumps and actual canopy disturbances can cause mismatches. Thus, we calculated indicators based on overlapping between reference polygons and disturbed patches instead of a conventional pixel-wise approach, as done by Aquino et al. (2022).

FLCD was applied on Mbe 2018-2019, Mbe 2021, Kab 2021, Kab 2020, Yan 2021, Dzg 2021 and Min 2021, resulting in seven binary disturbance maps. Detected disturbed pixels around roads, identified through aerial photographs, were reclassified as undisturbed using a buffer of 30 m. All GPS points that overlapped with the train dataset (i.e., UAV-derived binary forest disturbance map in Mbe 2018) were removed. For each forest disturbance map produced, the dates of detected disturbances were filtered to match with the year of GPS data. Reference polygons were computed by applying a buffer area of 20 m around the felled trees points. The resulting polygons were used to estimate the Logging gap Detection Rate (LDR) and Unconfirmed Detected Logging gap Rate (UDLR) defined as:

$$\text{LDR} = 100\frac{n_{\text{rp}}}{n_r} \text{ and } \text{UDLR} = 100\frac{(n_{\text{p}} - n_{\text{rp}})}{n_{\text{p}}} \tag{3}$$

Where n_r is the total number of reference polygons, n_p the number of detected patches and n_{rp} the number of detected patches overlapping reference polygons. In this patch based framework, n_{rp} is equivalent to true positives (TP) and n_p-n_{rp} to false positives (FP). The LDR metric is therefore related to TP, whereas the UDLR metric reflects FP. False negatives (FN) and true negatives (TN) have no equivalent metric, as the field measurements do not include information on undisturbed areas. The LDR index answers the question: "What is the rate of referenced logging gaps that are correctly detected?" whereas the UDLR index answers: "What is the rate of detected patches that do not correspond to logging gap events?". This process was implemented using the "vectorize", "patches", "extract" and "intersect" functions from the "terra" R package (Hijmans et al., 2022).

Finally, the discrepancy between detected and reference disturbance dates were analyzed. First, GPS reference polygons were rasterized on the basis of the detected disturbance maps grid (10 m resolution). The difference between reference and detected dates were computed on the overlapping disturbance pixels. The histogram, median, mean, first and third quartiles were calculated from the differences between dates for each study area.

2.8 Comparison with the cumulative sum approach

In this study, we developed a new method called FLCD. We compared its performances to that of the CuSum method, which is accessible and of proven effectiveness in detecting small-sized forest disturbances under 0.1 ha (i.e., 1,000 m^2 or 20 × 50 m). Since the RADD method was previously compared with CuSum (Aquino et al., 2022), and its minimum mapping unit is 0.1 ha, we do not compare it quantitatively with FLCD. Dupuis et al. (2023) also introduced an effective method for detecting small forest disturbances monthly, but do not aim to accurately predict felling dates. Finally, the study conducted by Carstairs et al. (2022) exhibits high potential for

measuring the extent of forest disturbances at 1 ha scale. However, they state that "the presence of geolocation errors and false alarms makes this method unsuitable for confirming individual disturbances". Although they found a linear relationship between the detected S-1 shadow and LiDAR-based canopy loss at a scale of 1 ha, they do not claim that their method could accurately identify individual disturbances or determine accurate logging dates.

Forest disturbance maps derived from the CuSum approach were computed using the open python code (https://github.com/chiaquino/S1_CuSum) provided by Aquino et al. (2022). To allow comparisons, both methods were applied to the same S-1 time series following data preprocessing described in Subsection 2.4. The CuSum method was also trained using the 2018-2019 UAV-derived binary forest disturbance map in the Republic of the Congo. A k-fold cross validation was used with the same five training and test datasets as FLCD varying the percentile at 95, 96, 97, 98, and 99. On this basis, the detection threshold was set to the 99th percentile of the CuSum maximum distribution (see the Supplementary Appendix S5.3 for details). The trained CuSum method was also validated on the extensive FSC and artisanal areas using the GPS point dataset and the 2019-2020 UAV map. Differences in LDR between FLCD and CuSum were assessed using a paired Wilcoxon signed-rank test from the LDR values computed on the height study sites. UDLR was not tested because it could only be computed for FSC-certified sites, resulting in an insufficient sample size for robust testing.

Both FLCD and CuSum share common features, as they rely on S-1 VV-polarized gamma nought SAR time series to detect small-scale canopy disturbances. Methodologically, both approaches identify significant decreases in the radar signal using percentile based detection thresholds and provide estimates of disturbance date and magnitude. FLCD explicitly models the temporal evolution of the SAR signal using fused-lasso regression, whereas CuSum is based on cumulative sums of residuals derived from the SAR signal. Disturbance dates in FLCD are derived from a sliding sum of negative local differences in the fused lasso regression. In contrast, CuSum relies on the maximum cumulative sum relative to the mean temporal signal. Finally, compared to CuSum, FLCD includes an additional post-classification spatiotemporal filtering step to remove isolated false detections.

3 Results

3.1 Training of the FLCD method on the UAV-covered area

Based on the 5-fold cross-validation approach, the sliding period size for the sliding sum was set to 3 months. The detection threshold was set as the 0.01th percentile of the distribution of all negative sliding sum values across the entire image. In other words, disturbances were identified when the summed negative values of the time series for a given pixel were more extreme than 99.99% of the corresponding values across all pixels, indicating significant forest structural change. The exclusion patch size during the post-classification process was set to 0.01 ha (i.e., one 10 m pixel corresponding to the pixel spacing of S-1). Therefore, the current trained FLCD method cannot reliably detect disturbances smaller than two adjacent 10 m pixels (i.e., 0.02 ha or 200 m^2). These disturbances may be detectable if, despite their small area, they significantly affect the S-1 signal in both pixels. This is because while the individual pixel spacing of S-1 is 10 m, its actual resolution is coarser (20 × 22 m).

Figure 4 shows the maps produced by the FLCD method with the calibrated parameters over the 2018-2019 UAV-derived binary forest disturbance map. Throughout the monitoring period (June 2018 - April 2019), the trained method reached a precision of 55% and a recall of 23.78% The majority of disturbance detections occurred in December 2018 and January 2019 (see Figure 4 Left panel) and corresponded to a 4–10 dB decrease in the VV signal (i.e., disturbance magnitude, see Figure 4 Right panel).

For illustration purposes, Figure 5 shows the temporal behaviors of γ^0 VV, fused-lasso regressions and sliding sum values on three classes of pixels with different profiles. The first class corresponds to actually disturbed pixels detected by the FLCD method (true positive rate), the second to undisturbed pixels misclassified as disturbed (false positive rate) and the last one corresponds to undetected real disturbances (false negative rate). When the FLCD method succeeds in detecting the disturbances (true positive rate), the SAR signal is relatively steady before and after the disturbance, which itself materializes as a decrease in the signal of varying time length and magnitude. This corresponds to horizontal fused-lasso regression lines interrupted by neatly decreasing segments. The sliding sum highlights the successive negative decreases. In the case of false positive rates, the FLCD method misclassified pixels as disturbed due to either a weak decrease in the SAR signal nevertheless exceeding the percentile threshold. Finally, the FLCD method failed to detect some disturbances (false negatives) which did not alter the signal stationarity leading to fused-lasso regressions remaining constant all over the series.

3.2 Validation of the FLCD method using tree felling locations and dates

The method was validated on the independent datasets made of felled trees locations in the FSC study areas. This led to a LDR of 31.08% (see Table 2). The method's effectiveness at detecting logging gaps varied across individual sites, with the LDRs ranging between 24.32% and 37.78% on FSC study areas (Table 2) and from 28.57% to 59.09% on the artisanal study areas (see Supplementary Appendix S5.6). The UDLR varies from 31.23% to 66.89% accross the FSC study areas (Table 2).

The FLCD method was able to estimate accurately and precisely the logging dates on the FSC study areas with the median of differences between real and detected dates ranging from −6 to −2 days depending on the study area (Figure 6). In artisanal study areas, the median was −3, −6 and −20 days on Yan, Dzg and Min, respectively.

3.3 Comparison of FLCD to CuSum

From FSC-certified areas, we found that the FLCD method systematically yielded more accurate and precise logging dates than the CuSum approach (see Figure 6). Indeed, distributions of temporal deviations between detected and reference dates across

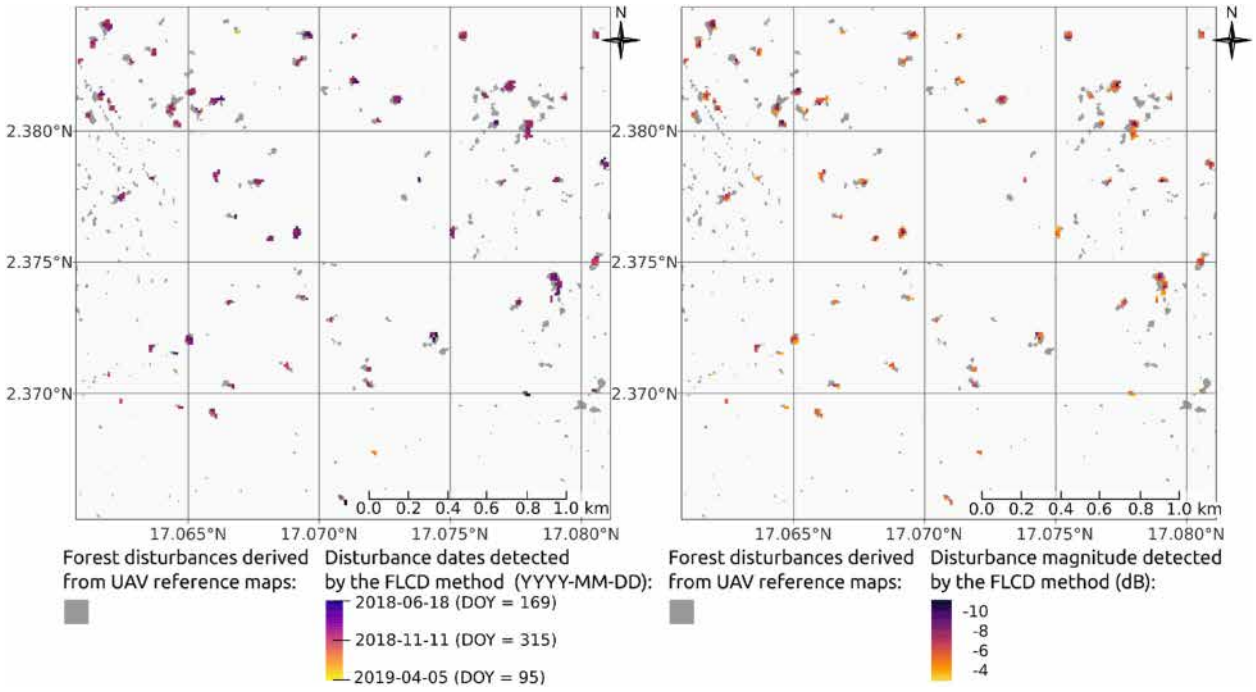

FIGURE 4
Results of the FLCD training on 2018-2019 UAV-derived binary forest disturbance map. The study area is located in the Republic of the Congo, on the Mbeti site (Mbe). The parameters of FLCD were calibrated using a 5-fold cross validation strategy. The left panel corresponds to the detected disturbance dates, and the right panel to the disturbance magnitude.

sites were larger with the CuSum than the FLCD method (Figure 6, see the Supplementary Appendix S5.6 for descriptive statistics values per study area). Concerning the smaller set of artisanal logging dates (see the Supplementary Appendix S5.6), results were contrasted across sites and fairly homogenous between methods with low bias and high precision on the Yan site (median ± sd: 0 ± 42.66 for CuSum and −3 ± 59.02 for FLCD), a moderate bias and low precision on the Dzg site (median ± sd: -29 ± 90.80 for CuSum and −6 ± 102.84 for FLCD) and a high bias on the Min site (median ± sd: -203 ± 89.65 for CuSum and −178 ± 75.63 for FLCD). Overall, LDR values of CuSum were slightly higher than those of FLCD across the five FSC-certified logging areas (i.e., three in Mbe and two in Kab, see Table 2). A similar pattern was observed on artisanal study areas (Dzg, Min, Yan) with CuSum systematically detecting 4 more logging gaps than FLCD (see the Supplementary Appendix S5.4). The paired Wilcoxon test indicated a statistically significant difference in LDR between FLCD and CuSum ($V = 2$, $p = 0.023$). On average, FLCD yielded lower LDR values than CuSum, with a median paired difference of −8.45%, indicating that CuSum detected a higher proportion of reference logging gaps. However, the confidence interval (−14.29% to −1.18%) also highlights the variability in relative performance across study sites. In FSC study areas, the number of unconfirmed logging gaps was overall high and higher for the Cusum than the FLCD method in three sites above five (see Table 2) ranging from 419 to 3,998 unconfirmed gaps for CuSum against 579 to 2,301 over-detected patches for FLCD. During the first UAV-covered period (2018–2019), which coincided with logging activities (n = 341 reference patches), UDLR were 10.61% and 9.52% for CuSum and FLCD, respectively. In the second period (2019–2020), when no logging occurred, the UAV map showed three disturbance patches likely caused by natural tree falls. During this period, CuSum and FLCD produced 17 and 61 false positives, respectively, with no overlap with the three reference patches.

From the UAV-covered reference area it was possible to analyze the detection rates in relation to the gap sizes (bearing in mind that this area was used for calibrating the two methods). Both methods agrees in displaying a sharp increase of true detections with gap size assessed from diachronic LiDAR (see Table 3). The detection rate was c. 49% for gap sizes of 0.02 ha and went above this value for larger gaps. It reached 71% and 90% for patches equal or higher than 0.05 and 0.20 ha, respectively The overlaps between detected and assessed patches also increased, albeit to a lesser extent, with FLCD yielding slightly higher overlap values. The results also highlighted that the gap size frequency distribution is overall skewed towards very small gaps with only 35% of LiDAR-assessed gaps equal or over 0.02 ha, and 9% equal or above 0.05 ha.

4 Discussion

Tropical forest degradation threatens forest-provided ecosystem services and biodiversity (Putz and Redford, 2010; Ghazoul et al., 2015). Although RIL and certification have proven effective in mitigating such degradation (Putz and Pinard, 1993), a large share of logging concessions remains uncertified. Moreover, informal or artisanal logging now represents the major share of

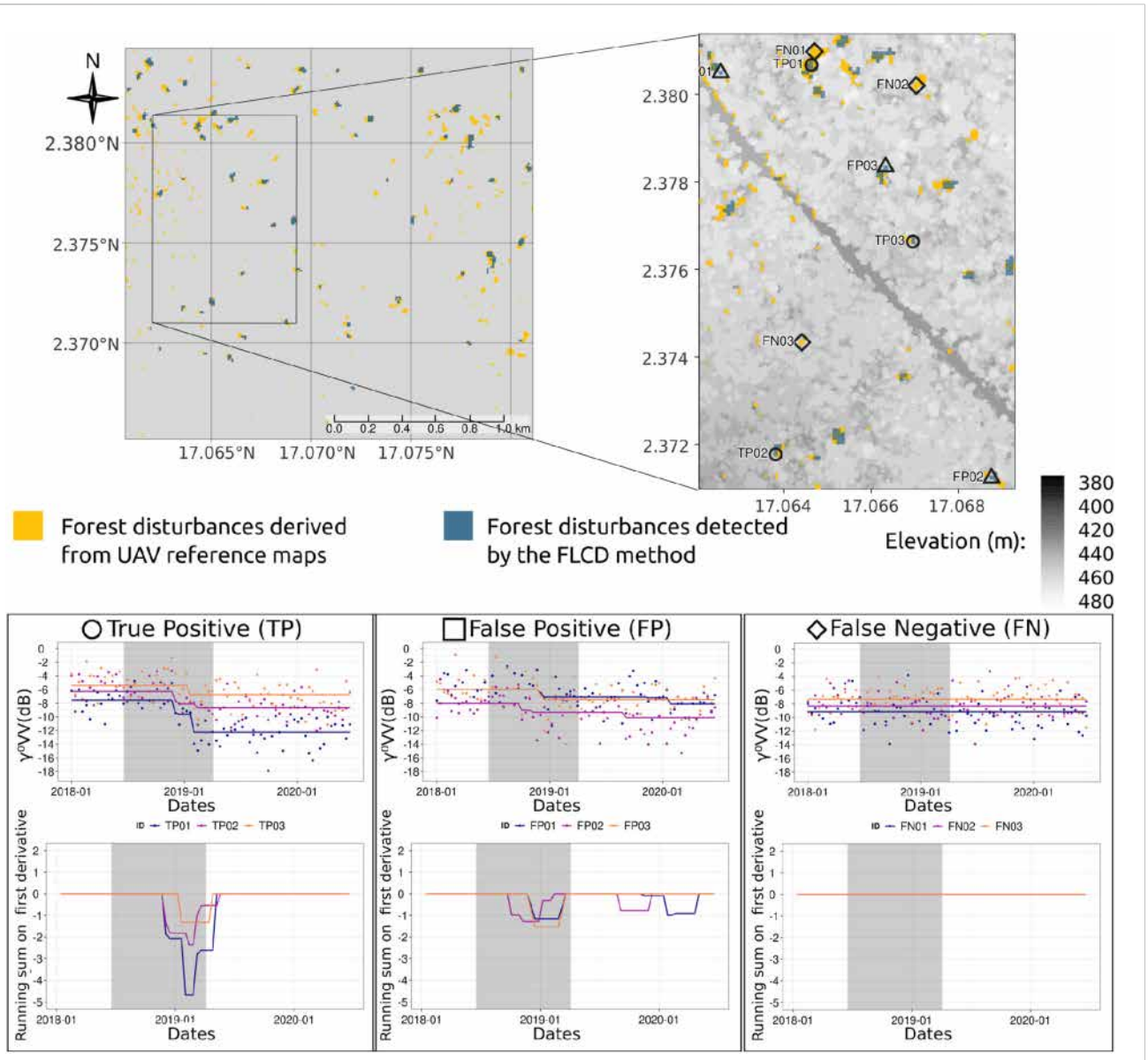

FIGURE 5
Examples of SAR temporal signatures leading to true positive (circle), false positive (square) and false negative (rhombus) detections during the training process. Top panels show the forest disturbances map calculated between 2018-06-18 and 2019-04-05 from the UAV-derived binary forest disturbance maps and the detected dates from the FLCD method. Intermediate panels show the γ^0VV signal (dots) and the corresponding fused-lasso regressions (line). Lower panels show the sliding sum on the first derivatives. The grey band corresponds to the known disturbance period.

forest logging in the Congo Basin (Lescuyer et al., 2025). Operational indicators on logging activities need to be devised and monitored as to assess logging impacts and drive timber harvesting towards more sustainable practices. High resolution maps of small-sized canopy disturbances associated to accurate estimates of disturbance dates can provide a sound basis to devise such operational indicators for logging monitoring (Dupuis et al., 2020). Early detection of advancing degradation fronts is particularly important, as these are often precursors to deforestation (Vancutsem et al., 2020).

4.1 Assessment of the FLCD method

The FLCD method appeared relevant to monitor small-sized forest disturbances such as canopy gaps made by tree felling in both FSC industrial and artisanal logging contexts. The dates of the detected forest disturbances were estimated with a very high accuracy on FSC sites (i.e., −8.37 to +4.60 days of difference on average between the estimated and the actual disturbance date, see the Supplementary Appendix S5.6. Part of the uncertainty in the detected date is due to the fact that the actual tree felling date can occur at any time between the date of the image in which the change is first visible and the date of the previous image in the time series. This is a problem already encountered and reported in previous studies (Reiche et al., 2018a). Moreover, some pixels can still be disturbed after the felling event by delayed mortality of remaining vegetation (Dalagnol et al., 2019). Considering those two sources of uncertainty, the assessment of disturbance dates appeared of high accuracy.

TABLE 2 Validation results of the FLCD and CuSum methods on the FSC study areas. LDR = logging gap detection rate, UDLR = unconfirmed detected logging gap rate computed from Equation 3. The sites correspond to Kabo (Kab) and Mbeti (Mbe) in the Republic of the Congo.

Study area	Year	Nb of test points	LDR		Nb of detected gaps		Nb of unconfirmed gaps		UDLR (%)	
			CuSum	FLCD	CuSum	FLCD	CuSum	FLCD	CuSum	FLCD
Kab	2021	3,779	30.88	24.32	3,010	2,471	1,464	1,249	48.63	50.55
Kab	2022	3,279	38.24	27.87	5,554	3,440	3,998	2,301	71.98	66.89
Mbe	2018	6,433	35.99	30.00	3,660	3,063	1,117	959	31.31	31.96
Mbe	2019	6,520	40.35	37.78	4,354	4,226	1,628	1,754	37.39	41.50
Mbe	2021	3,663	31.15	35.35	1,598	1,854	419	579	26.22	31.23

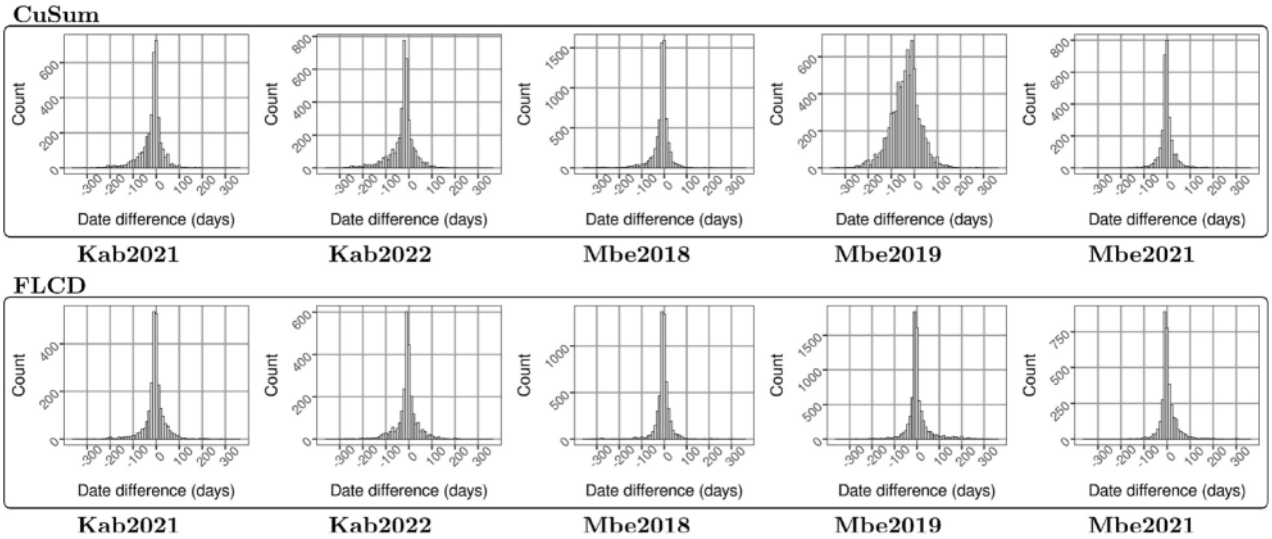

FIGURE 6
Histograms of differences (in days) between real and detected dates of tree felling for the CuSum (top row) and FLCD (bottom row) methods in the FSC study areas. The sites correspond to Kabo (Kab) and Mbeti (Mbe) in the Republic of the Congo.

TABLE 3 Validation of CuSum and FLCD according to minimum cluster size on the 2018–2019 UAV reference maps. "Minimum cluster size" is the minimum size of the UAV reference patches used for validation. "Nb of test patches" is the total number of reference patches derived from the UAV reference maps. "Nb of TP" is the percentage of UAV test patches overlapped by detected disturbances. "Total area" is the sum of the areas of the test patches. "Overlaps" corresponds to the percentage of overlap between the UAV reference disturbances and the predicted disturbed pixels.

Minimum	Nb of	Nb of TP (%)		Total area	Overlaps (%)	
Cluster size (ha)	Test patches	CuSum	FLCD	(ha)	CuSum	FLCD
0.00	341	19.65	18.77	9.90	16.69	20.78
0.01	260	33.33	32.69	8.80	18.24	22.85
0.02	126	49.20	48.41	7.98	20.24	25.32
0.03	92	61.79	62.41	7.09	22.07	27.10
0.05	56	71.42	71.43	5.72	24.92	30.58
0.10	20	90.00	90.00	4.04	29.05	36.78
0.20	4	100.00	100.00	1.05	33.16	39.88

Although our method targets canopy gaps as small as 0.02 ha (i.e., just two nominal S-1 pixels), our method detected an average of 31.1% of logging gaps in FSC sites (see Table 2) and 42.6% in artisanal logging areas (see the Supplementary Appendix S5.4). Moreover, detection results in the UAV-covered reference area clearly showed an increasing relationship of the detection rate with gap size, and they suggested that detection rates could be above 71% for canopy gaps in the range 0.05–0.1 ha (Table 3). These encouraging results remain however to be considered with caution and call for future verification on new UAV-based datasets of larger extent. Indeed, we assessed the parameters of the tested methods over our unique UAV-covered area of 374 ha, while our very large datasets from FSC concessions provide no information on the gap sizes associated to the felled tree locations. It is worth noting, however, that the rate of true positive we found in the UAV-covered area is very close to the rate observed in the FSC validation sites (32.9% vs. 31.1%), which suggests no blatant overfitting, as supported by the cross validation strategy implemented during calibration.

Considering false detections, the FSC datasets do not provide information on canopy disturbances apart from felled trees, whether natural tree fall gaps (i.e., chablis) or anthropogenic disturbances such as logging roads, log landing sites and even small-holder crops. As a result, all associated pixels are likely to be detected but incorrectly labeled as false positives, thereby inflating the UDLR figures. Indeed, UDLR values we observed in the FSC sites are high, i.e., ranging between 31.2% and 66.9% which is substantially greater than the 23% observed in the UAV-covered reference area, where we were able to accurately exclude canopy disturbances unrelated to tree felling. This supports the idea that a large fraction of the false positives registered in the FSC sites may well be actual gaps, though unrelated to logging or at least to tree felling operations. Additional UAV-borne data over large areas would be needed to accurately assess the fraction of actual gaps unrelated to logging, considering that this fraction seems to display notable inter-site and inter-annual variability. To get an idea, we may refer to studies on natural tree fall and deriving canopy gap creation. For instance, directly interpreting (Van Der Meer and Bongers, 1996) results suggests that the yearly proportion of standing tree that fall and actually create a canopy gap is about 1%, which would correspond to ca. 5 gaps/ha*year, compared to 0.5 to 4/ha tree felled in FSC concessions of Central Africa.

The observed UDLR values should thus be regarded as upper-limit estimates of false positives, which could be reduced using ancillary data to distinguish and sort out non-logging canopy gaps. Further research, though beyond the scope of the present paper could classify detected canopy disturbances by driver types in order to yield more accurate reference data to assess false positive values truly relating to small-area logging-induced disturbances (Dalagnol et al., 2023; Slagter et al., 2023).

4.2 Comparison between FLCD and CuSum

FLCD was more accurate than CuSum in estimating the dates of tree fellings. The discrepancy between the actual felling date and the detected disturbance date ranged from −8.34 to +4.60 days on average using FLCD and from −38.14 to +0.32 days on average using CuSum in the FSC sites (Mbe, Kab). Those last figures suggest an intrinsic bias of CuSum towards negative error values (i.e., estimated date posterior to the actual one), which seems also corroborated by site-wise figures. Overall, the detection rate obtained with CuSum was slightly higher than with FLCD: in some FSC-certified sites (Mbe), the LDR values showed modest differences but still significant based on the Wilcoxon test, while in others, somewhat more noticeable variations could be observed (Kab). In the UAV-covered area, both methods displayed very similar trends of increasing detection rate and precision with canopy gap sizes. Both yielded rates close to 71% for gaps of 0.05 ha. This suggests that observed detection rates might fundamentally reflect an intrinsic limit of the actual spatial resolution of the S-1 data that hinders detection of gaps of very small size (0.02–0.05 ha, i.e., just 2 to 5 pixels) whatever the method applied. Although S-1 data are provided at a ground spacing of 10 m, the effective spatial resolution after multilooking is coarser (approximately 20 × 22 m), which explains the reduced detection rates observed for disturbances close to the pixel size. This casts doubt on the feasibility of using S-1 data to track all individual felling events, since a large share of logging gaps are indeed very small and poorly detectable. Moreover, some gaps are retaining understorey vegetation cover or specific species such as palms in humid situations which could reduce the drop in S-1 signal. Having a large fraction of small logging gaps is in fact a positive result of FSC certification through improved felling techniques aimed at minimizing disturbances. In spite of these difficulties, both CuSum and FLCD can contribute effectively to monitoring logging activities and logging-induced degradation fronts at landscape scales. The UDLR rate quantifying detections that do not match referenced felling locations only showed weak differences between CuSum and FLCD bearing in mind the notable variability across FSC sites of results from both methods and considering the limited number of sites mentioning UDLR, to carry out a Wilcoxon test. The same explanations evoked for FLCD seem relevant to account for the large UDLR values also found for CuSum. The CuSum method is a threshold-based change detection method, while the FLCD is a trajectory segmentation method (Hirschmugl et al., 2017), which flexibility allows more improvement opportunities, considering the increasing availability of UAV-based data that will progressively help enhance training and parameter calibration. Indeed, regarding the flexibility of FLCD, longer time series could help improve the fused-lasso fitting (Tibshirani et al., 2005). Furthermore, in time series change detection methods, seasonal effects are often preliminarily suppressed from the remote sensing time series (Hirschmugl et al., 2017). Removing the seasonal effect from the S-1 signal can be done for both CuSum and FLCD methods as (Reiche et al., 2018b) did for RADD. However, the fused-lasso allows going further with the incorporation of external factors (Arnold et al., 2022) such as topography, season, month and dry-wet periods thereby helping remove a part of the signal noise as to better focus on forest changes. This opportunity to add external factors is further developed in the next Section 4.3 Prospects for improvement. In addition, our application included a post-classification step that was substantially reducing the number of commission errors (see the Supplementary Appendix S5.2) and could prove useful for other methods.

4.3 Prospects for improvement

Further studies should focus on improving the calibration of the FLCD method and on understanding how S-1-SAR characteristics contribute to the different types of detection errors. Firstly, FLCD (and also CuSum) is based on a percentile threshold (0.01 for FLCD and 99% for CuSum) calculated from all the pixels of the study area. Further research is needed to understand how integrating the properties of the land cover mosaic and the size of the study area to appropriately set this threshold. For instance, future work could investigate the sensitivity of the percentile-based detection threshold across contrasting landscape contexts, with varying forest-to-non-forest ratios. By optimizing threshold calculation such as choosing a minimum number of pixels in the study area and masking non-forests land uses, we may expect enhancing the accuracy of the felling gap detection. Secondly, based on a trajectory fitting approach (Hirschmugl et al., 2017), reference data (notably, multi-temporal UAV-borne) could be used to classify temporal S-1 signals that are characteristic of forest disturbances and sort out inappropriate signal trajectories that does not lend themselves to detecting punctual events (e.g., steadily decreasing ones as illustrated in Figure 5). These typical signal trajectories could be classified from fused-lasso regressions prior to going further into the threshold detection process. Indeed, the SAR signal variations induced by the speckle noise and local moisture fluctuations (Bouvet et al., 2018; Reiche et al., 2018b; Hirschmugl et al., 2020) increase the number of false positive detections. This is often handled through spatial smoothing. But Aquino et al. (2022) demonstrated that smoothing the time series using boxcar filters with a window of one to seven pixels systematically led to a decrease in the detection accuracy of the CuSum method. A major challenge in the tropics is the strong negative correlation between rain intensity and negative anomalies in the C-band SAR signal (Doblas et al., 2020), leading to false detections of forest disturbances. Finally, the incorporation of VH polarization has been suggested by Aquino et al. (2022) to improve the accuracy of the CuSum method as could also be done for FLCD. Although VH polarization is generally less sensitive than VV to abrupt canopy openings in dense tropical forests (Ygorra et al., 2021), it captures complementary scattering mechanisms related to volume scattering within the forest canopy. Previous studies have combined VV and VH information, or used derived indices such as VV/VH ratios, to help improve detection performance (Mermoz et al., 2021; Ygorra et al., 2021; Carstairs et al., 2022; Dupuis, 2023). Other SAR features, such as the radar vegetation index, polarimetric (Dupuis et al., 2020) and textural features (Balling et al., 2023; Hethcoat et al., 2021) have shown promising results in monitoring forest disturbances. The fused-lasso framework could be extended to incorporate SAR and external variables such as elevation, soil type, or location through a multi-type regularization approach. Devriendt et al. (2021) have presented a regression setting where different predictor types are assigned to penalty structures tailored to their specific properties. By modeling external variables to change gradually over time while allowing sudden changes in the forest signal itself, the FLCD method could better separate natural environmental effects from real logging events. For example, a drop in S-1 signal at low elevation may be likely due to human activity, while slow decrease at high elevation may reflect climatic stress. False positives could be reduced by incorporating contextual information into the fused-lasso framework by combining environmental covariates and spatial context. For example, the model could account for proximity to roads, clustering of detected disturbances, or elevation, helping to distinguish anthropogenic logging gaps from natural canopy openings. In addition, the launch of S-1C reduces the revisit interval compared to the 24-day period imposed by the loss of S-1B. This shorter revisit frequency can further improve the detection of small and short-term forest disturbances, because the growth of giant herbs and vines can be swift around the felled stumps. Moreover, even though the radar sensors are the most relevant in the humid tropics thereby reducing the gap size, complementary information can be expected from optical sensors, which for instance could be used to assess radar-detected gaps, as to reduce false positives. Indeed, while cloudiness hinders analyzing data series from optical sensors by limiting temporal regularity and frequency of usable images, a thorough analysis of such images, even if sparse, can help identify the nature and cause of the false positive. Those can be natural tree fall (rather small and isolated gaps), anthropogenic openings unrelated to tree felling (rather large and close to infrastructures), or genuine errors due to S-1 signal defects.

4.4 Prospects for logging and forest degradation monitoring

Tree felling, especially when unauthorized or unregistered tends to be at the forefront of the forest degradation process, which itself often pave the way to deforestation (Vancutsem et al., 2020). It is thus of importance to detect and delineate areas where new logging activities are initiated. Very often, such areas are not recognized and mapped as degraded by the current global monitoring systems (i.e., GLAD, TMF, RADD). We further note that for detecting felling gaps, both FLCD and CuSum have a clear edge against existing global monitoring methods such as GLAD (Hansen et al., 2016)/TMF (Vancutsem et al., 2020) and RADD alerts (Reiche et al., 2021), which do not pretend to address disturbances smaller than 0.09 and 0.1 ha, respectively. According to our field sites in Cameroon and the Democratic Republic of the Congo, 86% of the documented artisanal logging gaps were located in areas classified as “intact forest” in the TMF classification, while the median size of those documented gaps was ranging from 0.04 to 0.06 ha in the three sites. In a certified FSC concession in Aquino et al. (2022) found that only 2% of the logging-induced disturbances were detected by RADD against 59% by CuSum. In our FSC certified concessions, and as expected, RADD was able to detect only the larger forest disturbances in the UAV reference area (i.e., log landing sites and roads, see the Supplementary Appendix S5.7). In industrial logging concessions most of which are not certified, it is also needed to detect felling operations that may not respect the boundaries of annual coupes or the seasonal schedules that aim at soil protection. The method we propose here for detecting individual felling gaps is likely to highlight a surge of detections in any area experiencing new felling activities, even though a large share of felling events corresponds to individual gaps that are too small to be detectable from S-1 data. Such surges of spatially aggregated detections are clearly apparent in the dated detection maps presented in

Supplementary Appendix S5.5. Industrial logging operation are generally concentrated in time, and on a monthly or seasonally basis, the resulting spatial patterns of detected logging disturbances are unequivocally different from what could be expected from natural tree falls. Getting sufficiently accurate dates of canopy disturbance is here quintessential to monitor the displacement of logging operations by delineating areas in which logging activities are in progress and to verify whether they are in compliance with existing guidelines and regulations. Concerning the monitoring of informal or artisanal logging, we provide here the first hitherto results on the detectability of such activities through S-1 data. Although our dataset is modest compared to the massive sets provided by certified corporations, it enabled us to assess the proportion of detected trees among a set of recent felling sites that we thoroughly ascertained in the field in three distinct regions of Central Africa. Our study which is a first foray into the important question of measuring impacts of informal logging suggests that the detectability of canopy gaps made by artisanal logger may be at very similar levels than for logging corporations. Moreover, results are promising on two artisanal sites (Yan and Dzg) with histograms of date differences centered around zero as in the FSC sites (see the Supplementary Appendix S5.6). More comprehensive datasets, for instance based on UAV-borne diachronic LiDAR acquisitions are obviously needed to provide results on false detections. Regardless of the different logging types, the foreseeable increasing availability of such drone-borne datasets will provide a robust basis for consolidating the evaluation of the S-1-based gap detection techniques we attempted in the present study. Of course collecting UAV-borne data remains challenging in tropical areas of poor accessibility. However, difficulties are eased in industrial logging concessions where logging roads and camps allow accessing electricity sources for devices. Equipment costs for integrated UAV-Lidar systems are dwindling. Currently, once on the spot, a trained operator is able to cover about 1,000 ha in about 4 days of full work. For sampling a large logging concession, several sample patches of 1,000 ha each could be a good size. In addition to better evaluating false negatives and false positives, several avenues of investigation are possible as to draw more information from S-1 images. First, the spatiotemporal distribution of natural tree fall gaps should be compared with patterns of gaps generated by the different types of logging activities. Second, the spatial distribution of detected felling gaps is to be analyzed in relation to villages, road network and deforested areas. Thirdly, the return time of disturbances is a key parameter for evaluating forest degradation (Vásquez-Grandón et al., 2018) and disturbance detection could be repeated throughout the time series to detect recurring disturbances on the same pixel (or in neighboring pixels) and assess the closure time of the canopy by detecting when the signal returns close to its initial pre-disturbance value, as has been done in previous studies investigating forest recovery after wildfires and clear-cuts using optical satellite imagery (White et al., 2017; Chirici et al., 2020).

Regarding this third and last point, fused lasso regression constitutes a relevant framework for modeling and analyzing the temporal trajectories of the radar signal at the pixel scale. It will make it possible to take advantage of both the increasing availability of UAV-borne data and the lengthening of the S-1 image series to distinguish in the signal environmental and instrumental effects from those reflecting actual canopy changes.

Data availability statement

The DSM and forest disturbances derived from UAV acquisitions conducted in 2018, 2019 and 2020 in the Republic of the Congo are available on the CIRAD dataverse at https://doi.org/10.18167/DVN1/7RF7NF. The forest disturbance maps derived from the CuSum and FLCD methods in the five study areas in the Congo Basin are available on the CIRAD dataverse at https://doi.org/10.18167/DVN1/VM1OI1. The script of the Fused-Lasso Change Detection method is available on the CIRAD GitLab repository at https://gitlab.cirad.fr/forets-societes/projets/flcd.

Author contributions

AM: Writing – original draft, Writing – review and editing, Conceptualization, Data curation, Formal Analysis, Investigation, Methodology, Resources, Software, Validation, Visualization. JB: Writing – original draft, Writing – review and editing, Conceptualization, Funding acquisition, Investigation, Methodology, Project administration, Resources, Supervision, Visualization. FM: Writing – original draft, Writing – review and editing, Formal Analysis, Methodology, Software. NB: Writing – original draft, Writing – review and editing, Methodology, Resources. PP: Writing – review and editing, Methodology. GC: Writing – review and editing, Resources, Software. PC: Writing – original draft, Conceptualization, Funding acquisition, Investigation, Methodology, Project administration, Resources, Supervision, Visualization, Writing – review and editing.

Funding

The author(s) declared that financial support was received for this work and/or its publication. This research was funded through the PROFEAAC project funded by the French Development Agency (AFD) (AGREEMENT AFD No. CZZ 2123.01V) and the European Union – NextGenerationEU as part of the ARTISDIG research council of Finland project (decision number 348152). We thank Vincent Istace, Eric Forni and the consultants of the CIB SYLVAFRICA funded by the project DYNAFOR for providing the GPS points of felled trees and the UAV acquisitions over the FSC study areas. We also acknowledge support from the AfriCam project, funded by the French Development Agency (AFD) as part of PREACTS (PREZODE in Action in the Global south) program.

Acknowledgements

We thank Emilien Dubiez, Benjamin Hamisi, John Katembo and Jean-Claude Omba for their contributions in collecting field data in the Democratic Republic of the Congo. We thank Phillipe Guizol, Christian Fotso, Christian Tatchi, Essiane Edouard and J. G. Kayoum for their contribution in collecting field data in Cameroon. We thank local authorities and lumber men for their cooperation during the field campaigns in Cameroon and the Democratic Republic of the Congo. We thank Guillaume Lescuyer, Emilien Dubiez, Benjamin Hamisi and Phillipe Guizol for their contribution

in establishing the field protocols and preparing the field campaigns. We thank Sylvie-Gourlet Fleury, Valéry Gond and Maxime Réjou-Méchain for providing useful comments during the analysis. We thank Lilian Blanc for his comments on the manuscript. We thank Fabrice Bénédet for his help in depositing the data.

Conflict of interest

The author(s) declared that this work was conducted in the absence of any commercial or financial relationships that could be construed as a potential conflict of interest.

Generative AI statement

The author(s) declared that generative AI was not used in the creation of this manuscript.

Any alternative text (alt text) provided alongside figures in this article has been generated by Frontiers with the support of artificial intelligence and reasonable efforts have been made to ensure accuracy, including review by the authors wherever possible. If you identify any issues, please contact us.

Publisher's note

Supplementary material

The Supplementary Material for this article can be found online at: https://www.frontiersin.org/articles/10.3389/frsen.2026.1659305/full#supplementary-material

References

Antropov, O., Rauste, Y., Väänänen, A., Mutanen, T., and Häme, T. (2016). "Mapping forest disturbance using long time series of Sentinel-1 data: case studies over boreal and tropical forests," in 2016 IEEE International Geoscience and Remote Sensing Symposium (IGARSS), 3906–3909. doi:10.1109/IGARSS.2016.7730014

Aquino, C., Mitchard, E. T. A., McNicol, I. M., Carstairs, H., Burt, A., Puma Vilca, B. L., et al. (2022). Reliably mapping low-intensity forest disturbance using satellite radar data. *Front. For. Glob. Change* 5, 1018762. doi:10.3389/ffgc.2022.1018762

Arnold, T. B., Tibshirani, R. J., Arnold, M. T., and ByteCompile, T. (2022). Package 'genlasso. *Statistics* 39, 1335–1371. Available online at: https://CRAN.R-project.org/package=genlasso (Accessed August 20, 2024).

Asner, G. P., Keller, M., Pereira, R., Jr, Zweede, J. C., and Silva, J. N. (2004). Canopy damage and recovery after selective logging in Amazonia: field and satellite studies. *Ecol. Appl.* 14, 280–298. doi:10.1890/01-6019

Asner, G. P., Knapp, D. E., Broadbent, E. N., Oliveira, P. J. C., Keller, M., and Silva, J. N. (2005). Selective logging in the Brazilian Amazon. *Science* 310, 480–482. doi:10.1126/science.1118051

Balling, J., Herold, M., and Reiche, J. (2023). How textural features can improve SAR-based tropical forest disturbance mapping. *Int. J. Appl. Earth Observation Geoinformation* 124, 103492. doi:10.1016/j.jag.2023.103492

Banerjee, S. (2022). Horseshoe shrinkage methods for Bayesian fusion estimation. *Comput. Statistics & Data Analysis* 174, 107450. doi:10.1016/j.csda.2022.107450

Bouvet, A., Mermoz, S., Ballére, M., Koleck, T., and Le Toan, T. (2018). Use of the SAR shadowing effect for deforestation detection with Sentinel-1 time series. *Remote Sens.* 10, 1250. doi:10.3390/rs10081250

Bullock, E. L., Woodcock, C. E., and Olofsson, P. (2020). Monitoring tropical forest degradation using spectral unmixing and Landsat time series analysis. *Remote Sens. Environ.* 238, 110968. doi:10.1016/j.rse.2018.11.011

Bullock, E. L., Healey, S. P., Yang, Z., Houborg, R., Gorelick, N., Tang, X., et al. (2022). Timeliness in forest change monitoring: a new assessment framework demonstrated using Sentinel-1 and a continuous change detection algorithm. *Remote Sens. Environ.* 276, 113043. doi:10.1016/j.rse.2022.113043

Carstairs, H., Mitchard, E. T., McNicol, I., Aquino, C., Chezeaux, E., Ebanega, M. O., et al. (2022). Sentinel-1 shadows used to quantify canopy loss from selective logging in Gabon. *Remote Sens.* 14, 4233. doi:10.3390/rs14174233

Chirici, G., Giannetti, F., Mazza, E., Francini, S., Travaglini, D., Pegna, R., et al. (2020). Monitoring clearcutting and subsequent rapid recovery in mediterranean coppice forests with landsat time series. *Ann. For. Sci.* 77, 1–14. doi:10.1007/s13595-020-00936-2

Creese, A., Washington, R., and Jones, R. (2019). Climate change in the Congo Basin: processes related to wetting in the December–February dry season. *Clim. Dyn.* 53, 3583–3602. doi:10.1007/s00382-019-04728-x

Dalagnol, R., Phillips, O. L., Gloor, E., Galvão, L. S., Wagner, F. H., Locks, C. J., et al. (2019). Quantifying canopy tree loss and gap recovery in tropical forests under low-intensity logging using VHR satellite imagery and airborne LiDAR. *Remote Sens.* 11, 817. doi:10.3390/rs11070817

Dalagnol, R., Wagner, F. H., Galvão, L. S., Braga, D., Osborn, F., Sagang, L. B., et al. (2023). Mapping tropical forest degradation with deep learning and planet NICFI data. *Remote Sens. Environ.* 298, 113798. doi:10.1016/j.rse.2023.113798

Devriendt, S., Antonio, K., Reynkens, T., and Verbelen, R. (2021). Sparse regression with multi-type regularized feature modeling. *Insur. Math. Econ.* 96, 248–261. doi:10.1016/j.insmatheco.2020.11.010

DeVries, B., Verbesselt, J., Kooistra, L., and Herold, M. (2015). Robust monitoring of small-scale forest disturbances in a tropical montane forest using Landsat time series. *Remote Sens. Environ.* 161, 107–121. doi:10.1016/j.rse.2015.02.012

Doblas, J., Carneiro, A., Shimabukuro, Y., Sant'Anna, S., Aragão, L., and Pereira, F. R. S. (2020). Stabilization of Sentinel-1 sar time-series using climate and Forest structure data for early tropical deforestation detection. *ISPRS Ann. Photogrammetry, Remote Sens. Spatial Inf. Sci.* 2020, 89–96. doi:10.5194/isprs-annals-V-3-2020-89-2020

Dupuis, C., Lejeune, P., Adrien, M., and Fayolle, A. (2020). How can remote sensing help monitor tropical moist Forest Degradation? A systematic review. *Remote Sens.* 12, 1087. doi:10.3390/rs12071087

Dupuis, C., Fayolle, A., Bastin, J. F., Latte, N., and Lejeune, P. (2023). Monitoring selective logging intensities in central Africa with sentinel-1: a canopy disturbance experiment. *Remote Sens. Environ.* 298, 113828. doi:10.1016/j.rse.2023.113828

Dutrieux, L. P., Verbesselt, J., Kooistra, L., and Herold, M. (2015). Monitoring forest cover loss using multiple data streams, a case study of a tropical dry forest in Bolivia. *ISPRS J. Photogrammetry Remote Sens.* 107, 112–125. doi:10.1016/j.isprsjprs.2015.03.015

Food and Agriculture Organization of the United Nations (2020). Global forest resources assessment 2020: main report (Food & Agriculture Organization of the UN).

Forni, E., Rossi, V., Gillet, J.-F., Bénédet, F., Cornu, G., Freycon, V., et al. (2019). Dispositifs permanents de nouvelle génération pour le suivi de la dynamique forestiére en Afrique centrale: bilan en République du Congo. *Bois Forets Des Tropiques* 341, 55–70. doi:10.19182/bft2019.341.a31760

Ghazoul, J., Burivalova, Z., Garcia-Ulloa, J., and King, L. A. (2015). Conceptualizing forest degradation. *Trends Ecol. & Evol.* 30, 622–632. doi:10.1016/j.tree.2015.08.001

Goodbody, T. R., Coops, N. C., and White, J. C. (2019). *Digital aerial photogrammetry for updating area-based forest inventories: a review of opportunities, challenges, and future directions* 5. Springer, 55–75. doi:10.1007/s40725-019-00087-2

Gourlet-Fleury, S., Mortier, F., Fayolle, A., Baya, F., Ouédraogo, D., Bénédet, F., et al. (2013). Tropical forest recovery from logging: a 24 year silvicultural experiment from central Africa. *Philos. Trans. R. Soc. Lond. B Biol. Sci.* 368 20120302. doi:10.1098/rstb.2012.0302

Gourlet-Fleury, S., Rossi, V., Forni, E., Fayolle, A., Ligot, G., Allah-Barem, F., et al. (2023). Competition and site weakly explain tree growth variability in undisturbed central African moist forests. *J. Ecol.* 111, 1950–1967. doi:10.1111/1365-2745.14152

Grizonnet, M., Michel, J., Poughon, V., Inglada, J., Savinaud, M., and Cresson, R. (2017). Orfeo toolbox: open source processing of remote sensing images. *Open Geospatial Data, Softw. Stand.* 2, 1–8. doi:10.1186/s40965-017-0031-6

Hansen, M. C., Krylov, A., Tyukavina, A., Potapov, P. V., Turubanova, S., Zutta, B., et al. (2016). Humid tropical forest disturbance alerts using landsat data. *Environ. Res. Lett.* 11, 034008. doi:10.1088/1748-9326/11/3/034008

Hethcoat, M. G., Carreiras, J. M. B., Edwards, D. P., Bryant, R. G., and Quegan, S. (2021). Detecting tropical selective logging with C-band SAR data may require a time series approach. *Remote Sens. Environ.* 259, 112411. doi:10.1016/j.rse.2021.112411

Hijmans, R. J., Bivand, R., Forner, K., Ooms, J., Pebesma, E., and Sumner, M. D. (2022). *Package 'terra'*. Vienna, Austria: Maintainer. Available online at: https://CRAN.R-project.org/package=terra (Accessed August 20, 2024).

Hirschmugl, M., Gallaun, H., Dees, M., Datta, P., Deutscher, J., Koutsias, N., et al. (2017). Methods for mapping forest disturbance and degradation from optical Earth observation data: a review. *Curr. For. Rep.* 3, 32–45. doi:10.1007/s40725-017-0047-2

Hirschmugl, M., Deutscher, J., Sobe, C., Bouvet, A., Mermoz, S., and Schardt, M. (2020). Use of SAR and optical time series for tropical forest disturbance mapping. *Remote Sens.* 12, 727. doi:10.3390/rs12040727

Hoekman, D., Kooij, B., Quiñones, M., Vellekoop, S., Carolita, I., Budhiman, S., et al. (2020). Wide-area near-real-time monitoring of tropical forest degradation and deforestation using Sentinel-1. *Remote Sens.* 12, 3263. doi:10.3390/rs12193263

Jeon, J.-J., Sung, J. H., and Chung, E.-S. (2016). Abrupt change point detection of annual maximum precipitation using fused lasso. *J. Hydrology* 538, 831–841. doi:10.1016/j.jhydrol.2016.04.043

Kaçamak, B., Barbier, N., Aubry-Kientz, M., Forni, E., Gourlet-Fleury, S., Guibal, D., et al. (2022). Linking drone and ground-based liana measurements in a congolese forest. *Front. For. Glob. Change* 5, 803194. doi:10.3389/ffgc.2022.803194

Kleinschroth, F., Garcia, C., and Ghazoul, J. (2019). Reconciling certification and intact forest landscape conservation. *Ambio* 48, 153–159. doi:10.1007/s13280-018-1063-6

Lawson, S. (2014). Illegal logging in the democratic Republic of the Congo. *Energy, Environ. Resour. EER* 2014. Available online at: https://www.chathamhouse.org/sites/default/files/home/chatham/public_html/sites/default/files/20140400LoggingDRCLawson.pdf (Accessed August 8, 2024).

Lescuyer, G., Cerutti, P. O., and Robiglio, V. (2013). Artisanal chainsaw milling to support decentralized management of timber in central Africa? an analysis through the theory of access. *For. Policy Econ.* 32, 68–77. doi:10.1016/j.forpol.2013.02.010

Lescuyer, G., Vautrin, C., Mercier, A., Dubiez, E., Bisimwa, B., Betbeder, J., et al. (2025). Contribution of artisanal chainsaw milling to forest degradation in central Africa. *For. Trees Livelihoods* 35, 1–17. doi:10.1080/14728028.2025.2535578

Loubota Panzou, G. J., Ligot, G., Gourlet-Fleury, S., Doucet, J.-L., Forni, E., Loumeto, J.-J., et al. (2018). Architectural differences associated with functional traits among 45 coexisting tree species in central Africa. *Funct. Ecol.* 32, 2583–2593. doi:10.1111/1365-2435.13198

Mermoz, S., Bouvet, A., Koleck, T., Ballere, M., and Le Toan, T. (2021). Continuous detection of forest loss in Vietnam, Laos, and Cambodia using Sentinel-1 data. *Remote Sens.* 13, 4877. doi:10.3390/rs13234877

Nolan, S. (2022). *Utilising Sentinel-1 imagery to provide accurate detection of selective logging in the tropics*. The University of Edinburgh. doi:10.7488/era/2715

OFAC (2023). Observatoire des Forêts d'Afrique Centrale.

Pearson, T. R. H., Brown, S., Murray, L., and Sidman, G. (2017). Greenhouse gas emissions from tropical forest degradation: an underestimated source. *Carbon Balance Manag.* 12, 3. doi:10.1186/s13021-017-0072-2

Potapov, P., Hansen, M. C., Kommareddy, I., Kommareddy, A., Turubanova, S., Pickens, A., et al. (2020). Landsat analysis ready data for global land cover and land cover change mapping. *Remote Sens.* 12, 426. doi:10.3390/rs12030426

Putz, F. E., and Pinard, M. A. (1993). Reduced-impact logging as a carbon-offset method. *Conserv. Biol.* 7, 755–757. doi:10.1046/j.1523-1739.1993.7407551.x

Putz, F. E., and Redford, K. H. (2010). The importance of defining 'forest': Tropical forest degradation, deforestation, long-term phase shifts, and further transitions. *Biotropica* 42, 10–20. doi:10.1111/j.1744-7429.2009.00567.x

Putz, F. E., Sist, P., Fredericksen, T., and Dykstra, D. (2008). Reduced-impact logging: challenges and opportunities. *For. Ecol. Manag.* 256, 1427–1433. doi:10.1016/j.foreco.2008.03.036

Qin, Y., Xiao, X., Wigneron, J.-P., Ciais, P., Brandt, M., Fan, L., et al. (2021). Carbon loss from forest degradation exceeds that from deforestation in the brazilian amazon. *Nat. Clim. Chang.* 11, 442–448. doi:10.1038/s41558-021-01026-5

Reiche, J., Verbesselt, J., Hoekman, D., and Herold, M. (2015). Fusing landsat and SAR time series to detect deforestation in the tropics. *Remote Sens. Environ.* 156, 276–293. doi:10.1016/j.rse.2014.10.001

Reiche, J., Hamunyela, E., Verbesselt, J., Hoekman, D., and Herold, M. (2018a). Improving near-real time deforestation monitoring in tropical dry forests by combining dense Sentinel-1 time series with landsat and ALOS-2 PALSAR-2. *Remote Sens. Environ.* 204, 147–161. doi:10.1016/j.rse.2017.10.034

Reiche, J., Verhoeven, R., Verbesselt, J., Hamunyela, E., Wielaard, N., and Herold, M. (2018b). Characterizing tropical forest cover loss using dense Sentinel-1 data and active fire alerts. *Remote Sens.* 10, 777. doi:10.3390/rs10050777

Reiche, J., Mullissa, A., Slagter, B., Gou, Y., Tsendbazar, N.-E., Odongo-Braun, C., et al. (2021). Forest disturbance alerts for the Congo Basin using Sentinel-1. *Environ. Res. Lett.* 16, 024005. doi:10.1088/1748-9326/abd0a8

Réjou-Méchain, M., Mortier, F., Bastin, J.-F., Cornu, G., Barbier, N., Bayol, N., et al. (2021). Unveiling African rainforest composition and vulnerability to global change. *Nature* 593, 90–94. doi:10.1038/s41586-021-03483-6

Saha, N. (2021). "Tropical forest and sustainability: an overview," in *Life on land, encyclopedia of the UN sustainable development goals* (Switzerland: Springer), 1070–1078. doi:10.1007/978-3-319-95981-8_37

Scheffler, D., Hollstein, A., Diedrich, H., Segl, K., and Hostert, P. (2017). Arosics: an automated and robust open-source image co-registration software for multi-sensor satellite data. *Remote Sensing* 9, 676. doi:10.3390/rs9070676

Slagter, B., Reiche, J., Marcos, D., Mullissa, A., Lossou, E., Peña-Claros, M., et al. (2023). Monitoring direct drivers of small-scale tropical forest disturbance in near real-time with Sentinel-1 and -2 data. *Remote Sens. Environ.* 295, 113655. doi:10.1016/j.rse.2023.113655

Small, D. (2011). Flattening gamma: radiometric terrain correction for SAR imagery. *IEEE Trans. Geoscience Remote Sens.* 49, 3081–3093. doi:10.1109/TGRS.2011.2120616

Souza, C. M., Roberts, D. A., and Cochrane, M. A. (2005). Combining spectral and spatial information to map canopy damage from selective logging and forest fires. *Remote Sens. Environ.* 98, 329–343. doi:10.1016/j.rse.2005.07.013

Tang, X., Bratley, K. H., Cho, K., Bullock, E. L., Olofsson, P., and Woodcock, C. E. (2023). Near real-time monitoring of tropical forest disturbance by fusion of landsat, sentinel-2, and sentinel-1 data. *Remote Sens. Environ.* 294, 113626. doi:10.1016/j.rse.2023.113626

Tegegne, Y. T., Lindner, M., Fobissie, K., and Kanninen, M. (2016). Evolution of drivers of deforestation and forest degradation in the Congo Basin forests: exploring possible policy options to address forest loss. *Land Use Policy* 51, 312–324. doi:10.1016/j.landusepol.2015.11.024

Tibshirani, R. (1996). Regression shrinkage and selection *via* the lasso. *J. R. Stat. Soc. Ser. B Stat. Methodol.* 58, 267–288. doi:10.1111/j.2517-6161.1996.tb02080.x

Tibshirani, R., Saunders, M., Rosset, S., Zhu, J., and Knight, K. (2005). Sparsity and smoothness *via* the fused lasso. *J. R. Stat. Soc. Ser. B* 67, 91–108. doi:10.1111/j.1467-9868.2005.00490.x

Van Der Meer, P. J., and Bongers, F. (1996). Patterns of tree-fall and branch-fall in a tropical rain forest in French Guiana. *J. Ecol.* 84, 19–29. doi:10.2307/2261696

Vancutsem, C., Achard, F., Pekel, J.-F., Vieilledent, G., Carboni, S., Simonetti, D., et al. (2020). Long-term (1990-2019) monitoring of tropical moist forests dynamics. doi:10.1101/2020.09.17.295774

Vásquez-Grandón, A., Donoso, P. J., and Gerding, V. (2018). Forest degradation: when is a forest degraded? *Forests* 9, 726. doi:10.3390/f9110726

Webb, E. L. (1997). Canopy removal and residual stand damage during controlled selective logging in lowland swamp forest of northeast Costa Rica. *For. Ecol. Manag.* 95, 117–129. doi:10.1016/S0378-1127(97)00020-0

White, J. C., Wulder, M. A., Hermosilla, T., Coops, N. C., and Hobart, G. W. (2017). A nationwide annual characterization of 25years of forest disturbance and recovery for Canada using landsat time series. *Remote Sens. Environ.* 194, 303–321. doi:10.1016/j.rse.2017.03.035

Woodhouse, I., van der Sanden, J., and Hoekman, D. (1999). Scatterometer observations of seasonal backscatter variation over tropical rain forest. *IEEE Trans. Geoscience Remote Sens.* 37, 859–861. doi:10.1109/36.752204

Ygorra, B., Frappart, F., Wigneron, J. P., Moisy, C., Catry, T., Baup, F., et al. (2021). Monitoring loss of tropical forest cover from Sentinel-1 time-series: a CuSum-based approach. *Int. J. Appl. Earth Observation Geoinformation* 103, 102532. doi:10.1016/j.jag.2021.102532

Zhang, Y., Ling, F., Wang, X., Foody, G., Boyd, D., Li, X., et al. (2021). Tracking small-scale tropical forest disturbances: fusing the landsat and Sentinel-2 data record. *Remote Sens. Environ.* 261, 112470. doi:10.1016/j.rse.2021.112470